4. THE TROPICS—H. J. Diamond and G. D. Bell, Eds.

a. Overview—H. J. Diamond

This tropics section consists of five primary topics: 1) ENSO and the tropical Pacific; 2) the MJO; 3) TC activity for the 2007 season in seven basins: the North Atlantic, eastern North Pacific, northwest Pacific, north Indian and south Indian, South Pacific, and Australia; 4) ITCZ behavior in the Pacific and Atlantic basins; and 5) a new section on the Indian Ocean dipole.

The year was characterized by a transition to La Niña conditions that, while not developed until August, resulted in suppressed convection near the date line by early June. Therefore, La Niña–like impacts on the upper-tropospheric circulation were already evident during June–August across the subtropical South Pacific. At times, the patterns of tropical convection were strongly modulated by the MJO, which likely influenced the onset of La Niña.

The 2007 Atlantic hurricane season was near normal, and slightly more active than in 2006. In the North and south Indian Ocean Basins, the numbers and strength of the TCs were significantly above average and included a world record rainfall amount of 5,510 mm over a 3–8-day period associated with a TC in the south Indian Ocean Basin. A sidebar expanding on the extraordinary north Indian Ocean TC season, which featured two category 5 storms,[1] is included. In contrast, TC activity was significantly below average in the eastern North Pacific and northwest Pacific basins, and in the southwest Pacific and Australian regions.

A very strong positive phase of the Indian Ocean dipole was present during 2007, and its possible climate impacts are examined. This pattern likely contributed to the lack of a traditional La Niña signal in the Northern Hemisphere subtropics during the peak of the Atlantic hurricane season.

b. ENSO and the tropical Pacific—G. D. Bell and M. Halpert

ENSO is a coupled ocean–atmosphere phenomenon, and is the leading mode of interannual variability over the equatorial Pacific Ocean. Opposite phases of ENSO are called El Niño and La Niña. El Niño is a periodic warming of the central and east-central equatorial Pacific, which acts to strengthen convection in these regions and to suppress convection over Indonesia. Conversely, La Niña is a quasi-periodic cooling of the central and east-central equatorial Pacific, which acts to shut down convection in these regions and to enhance convection over Indonesia. These convection patterns extend more than half the distance around the globe, and are the main mechanism by which ENSO impacts the upper-tropospheric circulation.

NOAA defines El Niño and La Niña using the Niño-3.4 index, which measures area-averaged SST anomalies between 5°N–5°S, 170°–120°W. El Niño occurs when the 3-month running mean of the Niño-3.4 index (called the ONI) reaches +0.5°C, and La Niña occurs when the ONI reaches −0.5°C. Both phases of ENSO occurred during 2007. The Niño-3.4 index shows that a weak El Niño dissipated early in the year, and a moderate-strength La Niña developed late in the year (Fig. 4.1).

For the entire DJF 2006–07 season, the Niño-3.4 index averaged +0.8°C, which satisfied NOAA's definition for El Niño. Equatorial SSTs were generally +0.5° to +1.0°C above average between the date line and the west coast of South America during the period, with the largest departures (exceeding +1°C) centered near the date line and over portions of the eastern Pacific Ocean (Fig. 4.2a). Much of this anomalous warmth dissipated rapidly during January and February, with the weekly Niño-3.4 index returning to zero by mid-February.

During DJF the positive subsurface temperature anomalies were confined mainly to the region around the date line. These anomalies were weak (+1.0° to +2.0°C) and only extended to a depth of 100 m (Fig. 4.3a). Small negative anomalies were present across the equatorial Pacific Ocean at the thermocline depth, which is generally situated between 100 and 150 m as indicated by the depth of the 20°C isotherm (solid black line) in Fig. 4.3a. This pattern reflects a confinement of the anomalously warm water to the near-surface, and a shoaling of the thermocline in association with enhanced upwelling. These condi-

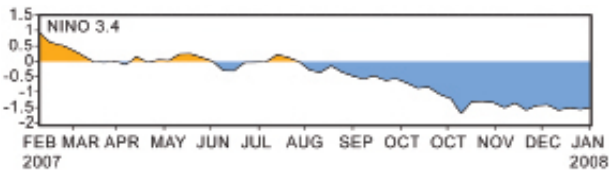

Fig. 4.1. Time series of SST anomalies (°C) in the Niño-3.4 region (5°N–5°S, 170°–120°W). Anomalies are departures from the 1971–2000 base period weekly means, and are obtained from the adjusted OI dataset (Smith and Reynolds 1998).

[1] Tropical cyclone categories are typically described using the Saffir–Simpson scale, and unless otherwise noted, category designations in this chapter will reflect Saffir–Simpson scale values (see www.nhc.noaa.gov/aboutsshs.shtml).

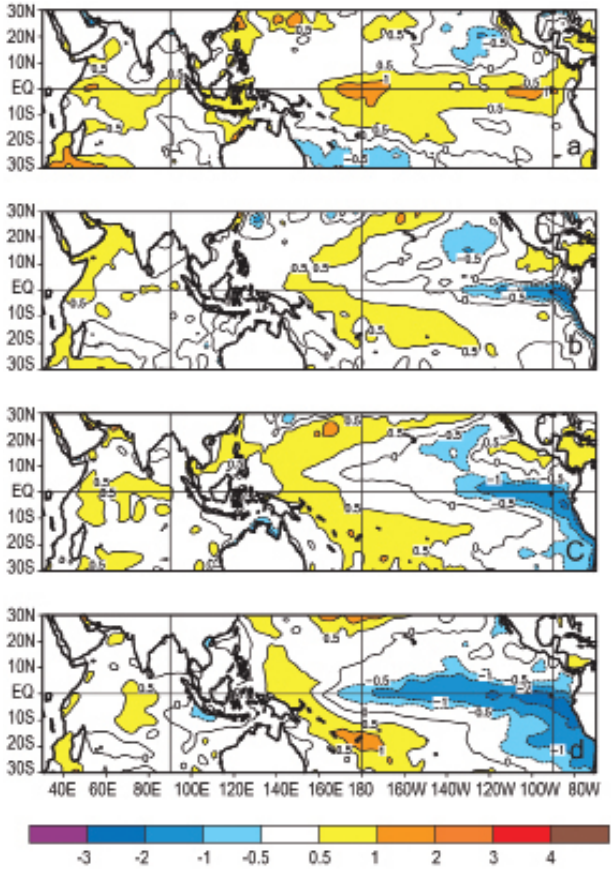

Fig. 4.2. SST anomalies (°C) during (a) Dec–Feb 2006–07, (b) Mar–May 2007, (c) Jun–Aug 2007, and (d) Sep–Nov 2007. Anomalies are departures from the 1971–2000 adjusted OI climatology (Smith and Reynolds 1998).

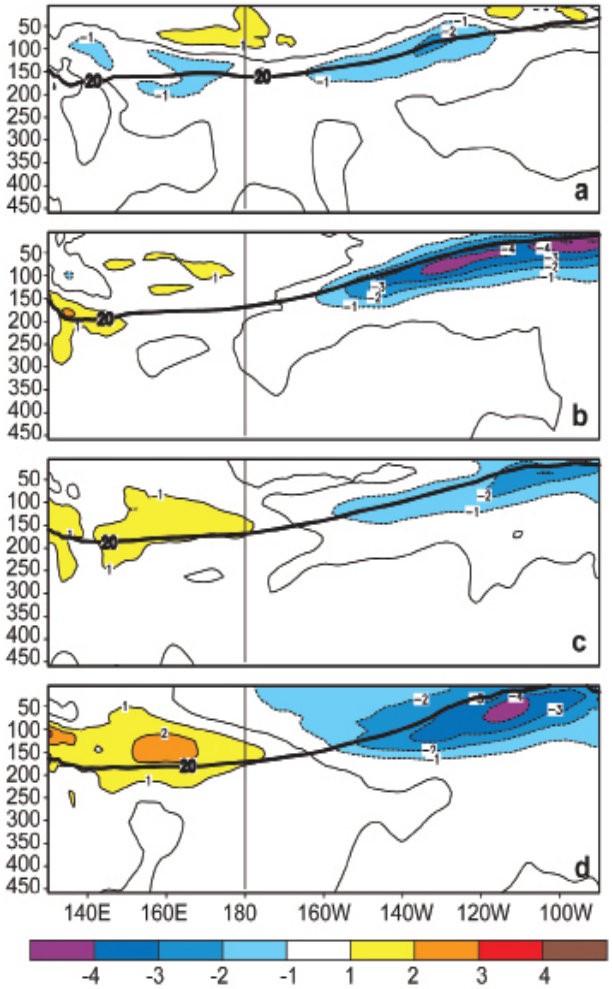

Fig. 4.3. Equatorial depth–longitude section of ocean temperature anomalies (°C) averaged between 5°N–5°S during (a) Dec–Feb 2006–07, (b) Mar–May 2007, (c) Jun–Aug 2007, and (d) Sep–Nov 2007. The 20°C isotherm (thick solid line) approximates the center of the oceanic thermocline. The data are derived from an analysis system that assimilates oceanic observations into an oceanic GCM (Behringer et al. 1998). Anomalies are departures from the 1971–2000 period monthly means.

tions were consistent with a weak and dissipating El Niño.

The patterns of anomalous tropical convection during DJF were also consistent with El Niño (shading, Fig. 4.4a). However, anomalous easterly winds at 850-hPa near the date line were not consistent with El Niño, and instead were associated with the increased oceanic upwelling. These easterly anomalies subsequently persisted throughout the year (Figs. 4.4b–d), and contributed to the drop in SST (Figs. 4.2b–d) and subsurface temperature (Figs. 4.3b–d) anomalies associated with the development of La Niña. By October–December, the value of the ONI had decreased to –1.2°C, indicating the strongest La Niña since 1999.

During key times of the year, the surface and subsurface temperature anomalies associated with ENSO were also strongly modulated by the MJO and its associated equatorial oceanic Kelvin wave activity (Figs. 4.7 and 4.8, section 4c). In December 2006, the upwelling phase of a strong Kelvin wave was triggered by an MJO and produced a sharp increase in upper-ocean heat content across the central and east-central equatorial Pacific. This was followed in January and early February by the upwelling phase of the wave, which contributed to El Niño's rapid demise (Fig. 4.8).

MJO activity also occurred during May–June, and the associated Kelvin wave activity may have delayed the onset of La Niña. For example, in June the downwelling phase of a Kelvin wave temporarily eliminated the negative heat content anomalies from

the entire eastern equatorial Pacific. The negative anomalies soon reappeared, but were interrupted by another Kelvin wave in early August. However, this impact was short-lived, and La Niña finally developed during August. During September–December, La Niña strengthened in association with a persistent pattern of suppressed convection and enhanced low-level easterly winds near the date line. Although the MJO and Kelvin wave activity were still present during this period, their impact on the oceanic heat content and SSTs was weaker, and mainly involved modulating the strength and westward extent of the negative anomalies associated with La Niña.

Although La Niña did not develop until late summer, suppressed convection was already established near the date line by early June (Fig. 4.5). Therefore, La Niña–like impacts on the upper-tropospheric (200 hPa) circulation were already evident during JJA across the subtropical South Pacific (Fig. 4.6a) (Kidson and Renwick 2002). These impacts included an extensive area of cyclonic anomalies across the subtropical South Pacific, and westerly wind anomalies (4–8 m s^{-1}) along the equator. Other impacts included easterly wind anomalies (4–12 m s^{-1}) across the eastern extratropical South Pacific, which reflected a marked westward retraction of the wintertime South Pacific jet stream and its associated jet exit region. As La Niña strengthened during SON, these anomalies became better defined and cyclonic anomalies also began to appear in the Northern Hemisphere subtropics near the date line (Figs. 4.6b).

By December, the La Niña signal was strongly influencing the upper-tropospheric circulation across the Pacific/North American sector. Impacts included a westward retraction of the wintertime East Asian jet stream. The downstream circulation features were also retracted westward, with a shift of the mean ridge from western North America to the central/eastern North Pacific, and a shift of the mean Hudson Bay trough to central and possibly western portions of North America. These conditions were associated with above average precipitation over much of the northern tier of the United States, and above-average temperatures in the southeast.

Regional La Niña impacts during 2007 included suppressed convection across the central and east-central equatorial Pacific, well above-average rainfall in South Africa during the first four months of

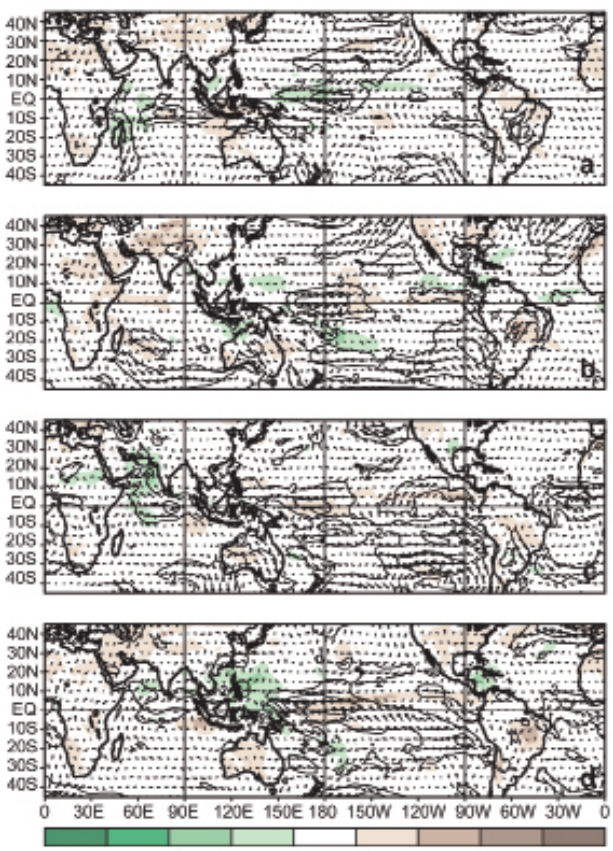

Fig. 4.4. Anomalous 850-hPa wind vector and speed (m s^{-1}) and anomalous outgoing longwave radiation (shaded, W m^{-2}) during (a) Dec–Feb 2006–07, (b) Mar–May 2007, (c) Jun–Aug 2007, and (d) Sep–Nov 2007. Anomalies are departures from the 1979–95 period monthly means.

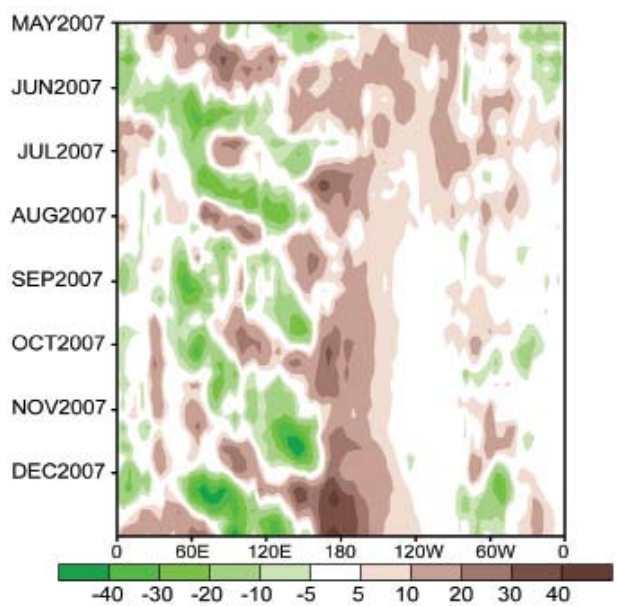

Fig. 4.5. OLR (W m^{-2}): (a) Time–longitude section of pentad anomalies between 5°N and 5°S. Green shading indicates enhanced convection, and brown shading indicates suppressed convection. Anomalies are departures from the 1979–2000 period means.

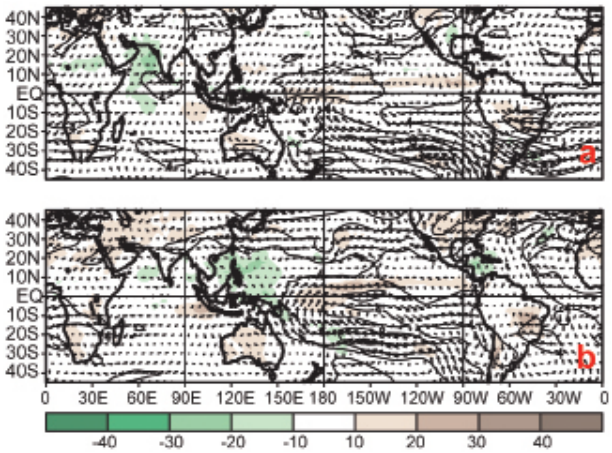

Fig. 4.6. Anomalous 200-hPa wind vector and speed (m s^{-1}) and anomalous OLR (shaded, W m^{-2}) during (a) Jun–Aug 2007, and (b) Sep–Nov 2007. Anomalies are departures from the 1979–95 period monthly means.

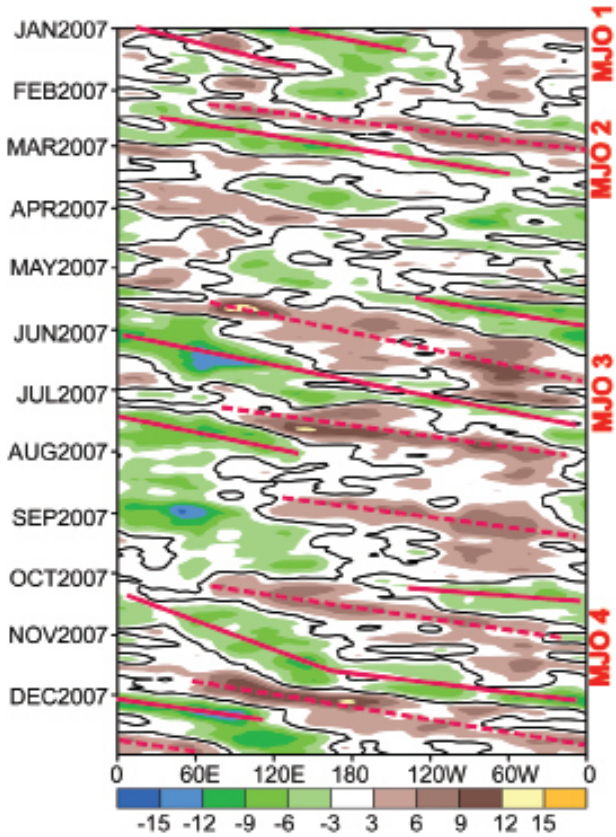

Fig. 4.7. Time–longitude section of 200-hPa velocity potential anomalies (5°N–5°S) for 2007. Green (brown) shading indicates anomalous divergence (convergence). Red lines highlight the MJO signal, and the four main periods of MJO activity are marked. Anomalies are departures from the 1971–2000 base period daily means.

the 2007–08 rainy season, increased storminess in the northwestern United States, and above-average temperatures across the southern tier of the United States. Another impact was the continuation of below average precipitation in the drought-stricken regions of northern Alabama, northern Georgia, and western North and South Carolina during the period from October to December. The SPCZ was displaced through ENSO activity, leading to regional rainfall anomalies over the southwest Pacific (see section 4d1).

c. The Madden–Julian Oscillation—J. Gottschalck and G. D. Bell

The MJO (Madden and Julian 1971, 1972, 1994) is a leading climate mode of tropical convective variability that occurs on intraseasonal time scales. The convective anomalies associated with the MJO often have the same spatial scale as ENSO, but differ in that they exhibit a distinct eastward propagation and generally traverse the globe in 30–60 days. The MJO can strongly affect the tropical and extratropical atmospheric circulation patterns, and sometimes produces ENSO-like anomalies (Mo and Kousky 1993; Kousky and Kayano 1994; Kayano and Kousky 1999). The MJO is often quite variable in a given year, with periods of moderate-to-strong activity sometimes followed by little or no activity. Overall, the MJO tends to be most active during neutral and weak ENSO periods, and is often absent during strong El Niño events (Zhang 2005; Zhang and Gottschalck 2002; Hendon et al. 1999).

The MJO is reflected in continuous propagation of 200-hPa velocity potential anomalies around the globe. A time–longitude section of this parameter shows four distinct periods during 2007 with at least moderate MJO activity (Fig. 4.7). These include 1) a strong event in January, 2) a short-lived event of moderate strength during late February and early March, 3) a long-lived event of moderate strength from May through early August, and 4) a strong event from late October through December.

The January event was a continuation of MJO activity that began in late 2006. That activity had previously triggered a strong equatorial oceanic Kelvin wave, whose upwelling phase and associated sharp drop in SSTs contributed to the rapid end of El Niño in early January. During January, enhanced equatorial convection associated with the MJO propagated eastward from Indonesia to the central Pacific Ocean, followed by an extended period of enhanced convection near the date line. These conditions were associated with anomalous easterly flow

and enhanced upwelling, which contributed to the drop in upper-ocean heat content in the east-central equatorial Pacific in February (Fig. 4.8).

The moderate-strength MJO activity during May through early August resulted in three distinct periods with below-average easterly winds near the date line. An oceanic Kelvin wave was triggered by the MJO during each of these periods (Fig. 4.8). Each wave was weaker than its predecessor, in part because of a gradual decrease in strength of the MJO. This Kelvin wave activity produced considerable intraseasonal variability in the SSTs and heat content across the central and east-central equatorial Pacific. In early June, the downwelling phase of a Kelvin wave eliminated the negative heat content anomalies in these regions. Significant cooling then ensued in late June as the upwelling phase of the wave propagated eastward. Another Kelvin wave produced a similar pattern of warming followed by cooling in late July and early August. This variability most likely delayed the onset of La Niña.

The strongest MJO event of the year began during October and lasted through December. This was the strongest and longest-lived event since March–June 2005. The 2007 event is somewhat unusual, in that MJO activity is typically reduced during La Niña. The resulting increased upwelling, which was linked to periods of enhanced easterly winds and the upwelling phases of oceanic Kelvin waves, acted to periodically reinforce the negative SST anomalies associated with La Niña. The MJO also periodically reinforced the La Niña–related pattern of tropical convection, as was seen in mid-December when exceptionally dry conditions spanned the central equatorial Pacific and exceptionally wet conditions covered Indonesia.

The MJO activity late in the year had two additional noteworthy impacts. It delayed the onset of the northwest Australia monsoon by 1–2 weeks in early December, and then strengthened that monsoon later in the month. The MJO also contributed to periods of intense storminess along the U.S. west coast during December and early January 2008, which produced heavy precipitation in central and Southern California that is not characteristically seen during La Niña.

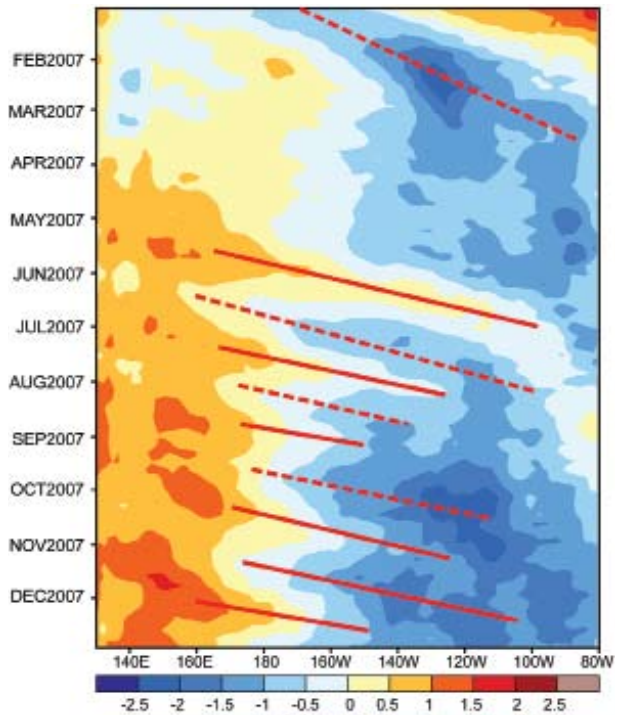

Fig. 4.8. Time–longitude section of anomalous upper ocean (0–300 m) heat content (5°N–5°S) during 2007. Blue (orange) shading indicates below (above) average heat content. The downwelling (solid) and upwelling (dashed) phases of oceanic Kelvin waves are indicated. Anomalies are departures from the 1982–2004 base period weekly means

d. Tropical cyclones

1) Overview—H. J. Diamond and D. H. Levinson

Averaged across all basins, the 2007 TC season (2006–07 in the Southern Hemisphere) saw a below normal (1981–2000 base) number of tropical or NS (≥34 kt) and HTC (≥64 kt), and significantly fewer major HTCs (≥96 kt) than average. Globally, 79 NSs developed during 2007 (18 below average), and 44 became HTCs (11 below average). Of these, only 18 (compared with 26 in 2006) attained major/intense status (average is 25.4). The global tallying of total storm numbers is always challenging, and involves more than simply adding up basin totals, as there are a number of storms that cross basin boundaries. Nonetheless, the overall numbers for the 2007 season were clearly below average.

The 2007 season was near normal in one basin (North Atlantic); significantly above average in two basins (NIO and SIO); and below average in the remaining basins (eastern North Pacific, northwest Pacific, southwest Pacific, and Australian). The SIO season saw twice the normal number of major TCs (6); while the NIO season featured two category 5 storms (Fig. 4.35), one of which was the strongest (and possibly first major TC) ever observed in the Arabian Sea. Both TCs caused considerable loss of life and extensive damage to the infrastructure of Oman, Iran, and Bangladesh (see sidebar article).

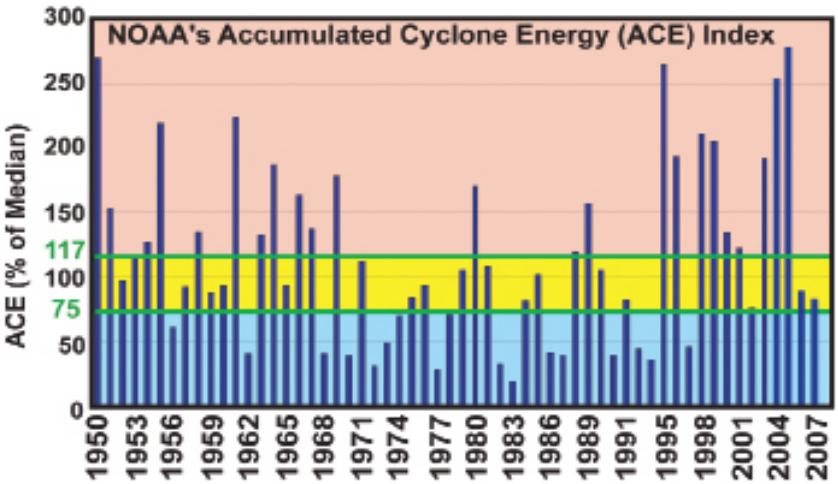

Fig. 4.9. NOAA's ACE index expressed as percent of the 1951–2000 median value (87.5×10^4 kt^2). ACE is a wind energy index that measures the combined strength and duration of the NSs. ACE is calculated by summing the squares of the 6-hourly maximum sustained wind speed in kts (Vmax^2) for all periods while the named storm has at least TS strength. Pink, yellow, and blue shadings indicate NOAA's classifications for above-, near-, and below-normal seasons, respectively.

2) Atlantic basin—G. D. Bell, E. Blake, C. W. Landsea, S. B. Goldenberg, R. Pasch, and T. Kimberlain

(i) Seasonal activity

The 2007 Atlantic hurricane season produced 15 NSs, 6 Hs and 2 MHs. The 1951–2000 averages are 11 NSs, 6 Hs, and 2 MHs. For 2007 the ACE index (Bell et al. 2000), a measure of the season's overall activity, was 84% of the 1950–2000 median (87.5 ¥ 10^4 kt^2) (Fig. 4.9). This value is in the near-normal range (see www.cpc.noaa.gov/products/outlooks/background_information.shtml) and reflects fewer and generally shorter-lived hurricanes and MHs compared to recent years.

Two hurricanes made landfall in the Atlantic basin during 2007 with category 5 strength. MH Dean struck the Yucatan Peninsula near Costa Maya on 21 August with 150-kt sustained winds. MH Felix then made landfall near Punta Gorda, Nicaragua, on 2 September with 140-kt sustained winds. In addition, several other TSs and Hs struck the region around the Caribbean Sea. The United States was struck by one H, one NS, and three TD. This represented an increase in landfalling storms compared to 2006 (which had NS landfalls), even though both seasons had similar ACE index levels.

(ii) Atmospheric conditions

The peak months (ASO) of the season featured a persistent TUTT (also called the midoceanic trough) over the central North Atlantic and MDR [indicated by the green box spanning the tropical Atlantic and Caribbean Sea between 9.5°–21.5°N and 20.0°–80.0°W (Goldenberg and Shapiro 1996)] (Fig. 4.10). The period also featured a strong and persistent ridge over eastern North America.

During August and September, these conditions produced above-average vertical wind shear (Figs. 4.11a,c) and anomalous midlevel sinking motion (Figs. 4.11b,d) across the western half of the MDR, Gulf of Mexico, and the western and central subtropical North Atlantic. As a result, extensive areas were unfavorable for hurricane development and intensification.

These conditions include below-average vertical wind shear (the difference between the 200- and 850-hPa winds), above-average SSTs, and enhanced convection. However, the pressure pattern in the lower atmosphere was not particularly conducive to hurricane formation. The main area of low pressure was located over the northwestern Caribbean Sea and Central America, with much of the circulation located over land. The pronounced northward shift of this feature, which is normally situated over the southern Caribbean Sea, is likely to have suppressed TC formation in that region.

For the entire ASO period, the primary area of weak vertical wind shear (less than 8 m s^{-1}) was confined mainly to the extreme southern MDR and western Caribbean Sea (shaded regions, Fig. 4.12a).

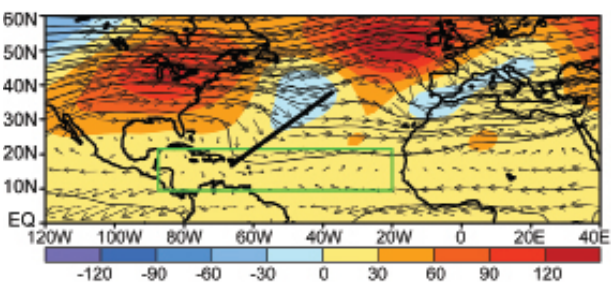

Fig. 4.10. Aug–Oct 2007: 200-hPa heights (contours, m), height anomalies (shaded), and vector winds (m s^{-1}). Thick solid line indicates the upper-level trough axis. Green box denotes the MDR. Anomalies are departures from the 1971–2000 period monthly means.

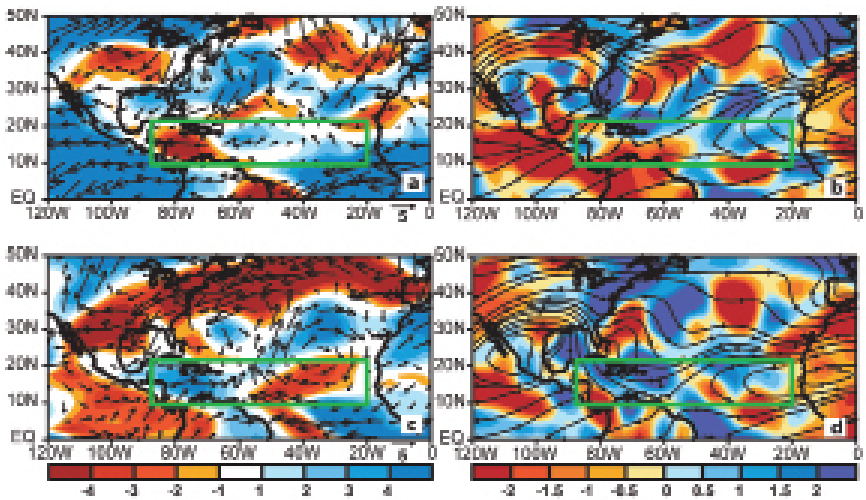

Fig. 4.11. (a),(c) The anomalous 200–850-hPa vertical wind shear strength (m s^{-1}) and vectors during (a) Aug and (c) Sep 2007. Red (blue) shading indicates below-average (above average) strength. (b),(d) The total 200-hPa streamlines and anomalous 500-hPa vertical motion (shaded) during (b) Aug and (d) Sep 2007. Red (blue) indicates anomalous ascent (descent). Green box denotes the MDR. Anomalies are departures from the 1971–2000 period monthly means.

This pattern was especially pronounced in August, when category 5 Hs Dean and Felix developed. Interestingly, the mean ASO vertical wind shear was below average across much of the MDR during ASO, which would normally suggest an above-normal season (Fig. 4.12b). However, for the eastern half of the MDR, most of the contribution to the negative anomalies came from October, a month when the total vertical shear is too strong to support TS formation.

It should be noted that improvements in tools such as QuikSCAT, and the AMSU, cyclone phase space, and the unique use of aircraft observations have likely led to more NSs and subtropical storms being identified now compared to a generation ago (Landsea 2007). For 2007, it is estimated that four NSs, Andrea, Chantal, Jerry, and Melissa, may not have been named a generation ago (Landsea 2007).

(iii) SSTs

SSTs in the MDR were above average (+0.27°C) during ASO 2007 (Fig. 4.13). This ongoing warmth since 1995 is associated with the warm phase of the AMO (Enfield and Mestas-Nuñez 1999) and the active Atlantic phase of the tropical multidecadal signal (Bell and Chelliah 2006). Some of the persistent warmth has also been linked to increasing global temperatures over the last 100 yr (Santer et al. 2006).

The above average SSTs during ASO 2007 were concentrated in the western half of the MDR, where departures averaged +0.47°C. The near-normal hurricane activity in these regions is not consistent with this ongoing warmth. Instead, it reflects the dominant role played by the atmospheric anomalies in controlling Atlantic hurricane activity (Shapiro and Goldenberg 1998). In the eastern MDR, SSTs cooled to near normal during ASO 2007. However, these cooler SSTs cannot account for the strong TUTT and upstream ridge in August and September or for the reduced Caribbean activity in October.

(iv) Prevailing global climate patterns

The occurrence of La Niña during an active hurricane era has been shown to significantly increase the probability of an above-normal Atlantic hurricane season,

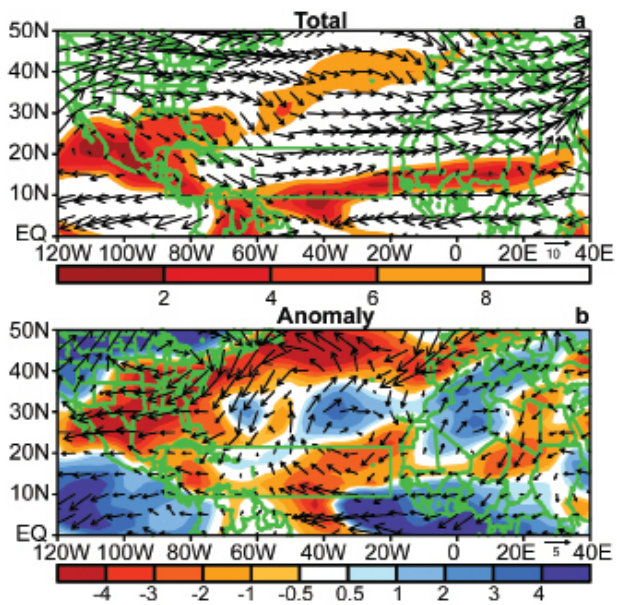

Fig. 4.12. Aug–Oct 2007: 200–850-hPa vertical wind shear magnitude (m s^{-1}) and vectors (a) total and (b) anomalies. In (a), shading indicates vertical wind shear below 8 m s^{-1}. In (b), red (blue) shading indicates below- (above) average magnitude of the vertical shear. Green box denotes the MDR. Vector scale is shown at bottom right of each panel. Anomalies are departures from the 1971–2000 period monthly means.

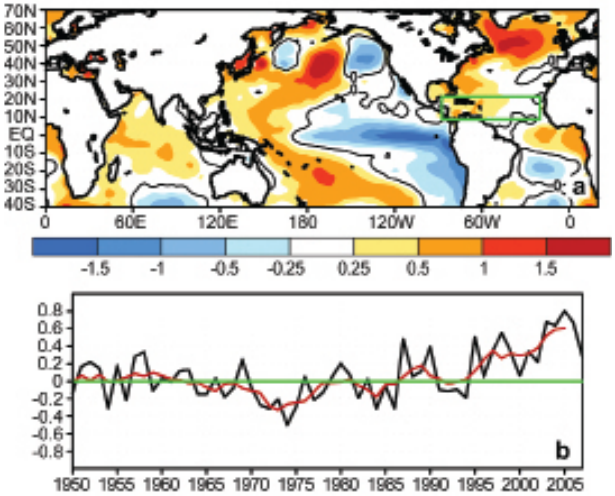

Fig. 4.13. (a) SST anomalies (°C) during Aug–Oct 2007. (b) Consecutive ASO values of SST anomalies in the MDR. Red line shows the corresponding 5-yr running mean. Green box in (a) denotes the MDR. Anomalies are departures from the 1971–2000 period monthly means.

in part because it typically produces a weaker TUTT and reduced vertical wind shear in the MDR (Gray 1984; Bell and Chelliah 2006). La Niña developed during August 2007, and subsequently reached moderate strength during September–November. Also, key atmospheric anomalies known to be associated with the current active hurricane period were in place as expected (section 2ivb).

(a) La Niña

Despite the strengthening La Niña during ASO 2007, its typical impacts on the upper-tropospheric circulation across the tropical North Pacific and MDR were notably absent (Fig. 4.14). Over the North Pacific, the 200-hPa streamfunction anomalies were weak, and the typical core of negative anomalies near the date line was absent. Also, there was a lack of persistent positive velocity potential anomalies near the date line, even though convection was suppressed throughout the region (Fig. 4.7). As a result, the downstream TUTT exhibited no connection to La Niña.

One suggested reason for this discrepancy is that convection over Indonesia and the eastern tropical Indian Ocean was also suppressed throughout the period (Fig. 4.15a). Negative streamfunction anomalies (indicating a weaker upper-level ridge) across the western subtropical North Pacific were consistent with this suppressed convection. These conditions are opposite to the typical La Niña signal, and in-

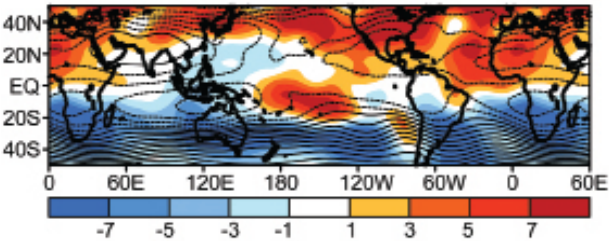

Fig. 4.14. Aug–Oct 2007: 200-hPa streamfunction (contours, interval is 10 x 106 m^2 s^{-1}) and anomalies (shaded). Anomalous ridges are indicated by positive values (red) in the NH and negative values (blue) in the SH. Anomalous troughs are indicated by negative values in the NH and positive values in the SH. Anomalies are departures from the 1971–2000 period monthly means.

dicate that the total La Niña forcing and resulting 200-hPa circulation anomalies were much weaker than would normally be expected for the observed Pacific cooling.

These conditions were associated with a record-strength pattern (Fig. 4.15b) that also included enhanced convection over the western equatorial Indian Ocean and enhanced convection across India and the Southeast Asian monsoon regions. This entire pattern is more typical of El Niño, as was seen in 2006. This climate signal may have overwhelmed the 200-hPa circulation anomalies normally associated with

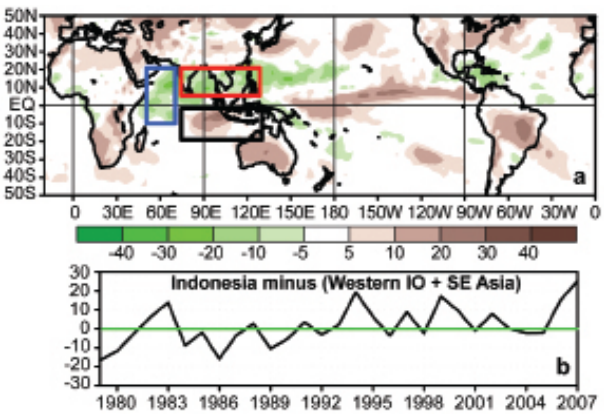

Fig. 4.15. Aug–Oct: (a) anomalous OLR (W m^{-2}), with green shading indicating enhanced convection, and brown shading indicating suppressed convection. (b) OLR time series based on boxed regions shown in (a). The time series is calculated as the area-averaged anomalies over Indonesia (black box) minus area-averaged anomalies over western IO (blue box) minus area-averaged anomalies over southeastern Asia (red box). Anomalies are departures from the 1979–2000 period monthly means.

La Niña, thus negating La Niña's normally enhancing influence on the 2007 Atlantic hurricane season. Conversely, this same pattern may have enhanced El Niño's suppressing influence on the 2006 Atlantic hurricane season (Bell et al. 2007).

(b) Conditions associated with the ongoing active Atlantic hurricane era

Although 2007 had about average activity, it was still more active than most seasons during the below-normal era 1971–94 (Fig. 4.9). A main contributing factor to the current active era is the tropical multidecadal signal, which reflects the leading modes of tropical convective rainfall variability occurring on multidecadal time scales (Bell and Chelliah 2006). A phase change in the tropical multidecadal signal corresponds with the dramatic transition in 1995 to the active era (Bell et al. 2007). Time series of key atmospheric wind parameters highlight the dramatic differences between these above-and below-normal hurricane eras (Fig. 4.16).

One key aspect of the current active hurricane era is an east–west oscillation in anomalous tropical convection between the West African monsoon region and the Amazon basin, signaling an enhanced West African monsoon system (Landsea and Gray 1992; Goldenberg and Shapiro 1996) and suppressed convection in the Amazon basin. A second aspect is ongoing above average SSTs in the North Atlantic, consistent with the warm phase of the Atlantic multidecadal mode (Goldenberg et al. 2001).

As shown by Bell and Chelliah (2006), these conditions are associated with an interrelated set of convectively driven atmospheric anomalies known to favor active hurricane seasons (Fig. 4.16). Most of these anomalies were again in place during 2007, including 1) enhanced ridging at 200 hPa in both hemispheres over the Atlantic Ocean (Fig. 4.14), 2) an enhanced tropical easterly jet and a westward expansion of the area of anomalous easterly winds at 200 hPa, 3) reduced tropical easterlies at 700-hPa across the central and eastern Atlantic (Fig. 4.16, middle), and 4) enhanced cyclonic relative vorticity along the equatorward flank of the African easterly jet (Fig. 4.16, bottom). In light of these ongoing conditions, there is no indication the current active hurricane era has ended.

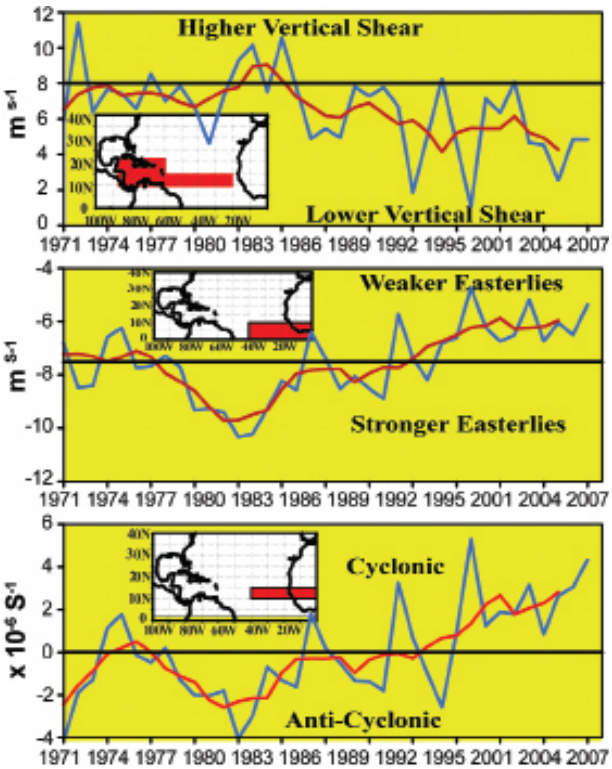

Fig. 4.16. Aug–Oct time series showing area-averaged values of (top) 200–850-hPa vertical shear of the zonal wind (m s^{-1}), (middle) 700-hPa zonal wind (m s^{-1}), and (bottom) 700-hPa relative vorticity (x 10^{-6} s^{-1}). Blue curve shows unsmoothed 3-month values, and red curve shows a 5-point running mean of the time series. Averaging regions are shown in the insets.

3) Eastern North Pacific basin—D. H. Levinson and J. Weyman

(i) Seasonal activity

The ENP basin includes two regions officially designated by NOAA's NWS for issuing NS and H warnings and advisories. The eastern Pacific warning area extends from the west coast of North America to 140°W and is the responsibility of NOAA's NHC in Miami, Florida, while the central Pacific warning area between 140°W and 180° is the responsibility of NOAA's CPHC in Honolulu, Hawaii. The 2007 TC activity in both these warning areas is covered using combined statistics, along with information summarizing activity and impacts in the central North Pacific region.

The ENP hurricane season officially lasts from 15 May to 30 November. The peak activity for the central (eastern) part of the region normally occurs in August (September). The 2007 ENP hurricane season produced 11 NSs, 4 Hs, and 1 MH (Fig. 4.17a). These values are well below the 1971–2005 averages, which are 16.2 NSs, 9.1 Hs, and 4.3 MHs. Four TDs also formed in the ENP during 2007 (03E, 04E, 05E, and 13E).

The 2007 season began quickly with two NSs in May (Alvin and Barbara), which has only happened twice before (1956 and 1984). However, the numbers of NSs and Hs were below normal in all subsequent

months. As a result, the seasonal ACE Index (Bell et al. 2000; Bell and Chelliah 2006) was only 52.7 × 10^4 kt^2, which is less than half of the 1971–2005 mean (126.3 × 10^4 kt^2), and the second lowest value (following 1977) since reliable records began in 1970 (Fig. 4.17b).

Only two systems (Cosme and Flossie) were observed in the central North Pacific region during 2007, which is also well below the 1971–2005 average of 4–5 TCs.[2] These storms both entered the region from the east.

(ii) Historical context of the 2007 ENP hurricane season

Since 1995, the numbers of NSs in the ENP basin has been near average, fluctuating around the long-term mean (Fig. 4.17a). However, the numbers of Hs and MHs have been generally below normal, with above normal H activity seen in only two seasons (2000 and 2006). NOAA has identified 8 of the 13 ENP seasons during 1995–2007 as being below normal, with only the 1997 and 2006 El Niño–influenced seasons producing above normal activity as measured by the ACE index. In contrast, higher activity seen during the preceding 1970–94 period, had 6 of 25 (24%) below normal seasons and 9 of 25 (36%) above normal seasons as measured by the ACE index.

These active and inactive ENP eras are opposite to those observed over the North Atlantic. Such east–west oscillations in activity reflect the large-scale atmospheric circulation anomalies that extend across both basins (Bell and Chelliah 2006). The spatial scale of these atmospheric anomalies is far larger than the area of warmer Atlantic SSTs (Lander and Guard 1998; Landsea et al. 1998, 1999; Goldenberg et al. 2001), suggesting this warmth alone is not a primary direct cause for the 1995 transition to generally below normal (above normal) ENP (Atlantic) hurricane seasons.

[2] NOAA's CPHC includes TDs in their climatological statistics for the central North Pacific region.

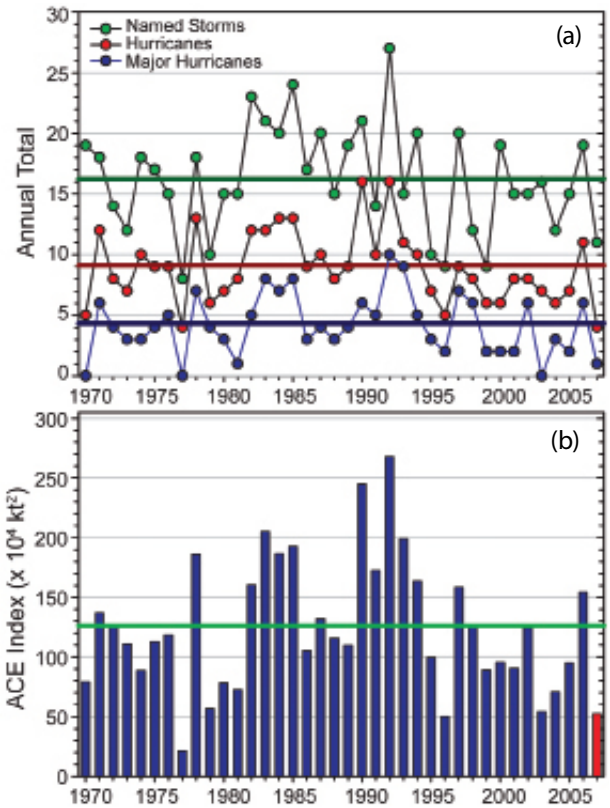

Fig. 4.17. Seasonal TC statistics for the east North Pacific Ocean during 1970–2007: (a) number of NS, H, and MH and (b) the ACE Index (x 10^4 kt^2) with the seasonal total for 2007 highlighted in red. Both time series include the 1971–2005 base period means.

(iii) Environmental influences on the 2007 hurricane season

Seasonal TC activity (both frequency and intensity) in the ENP basin is influenced by several large-scale environmental factors, including SSTs, 200–850-hPa vertical wind shear, the phase of the ENSO in the equatorial Pacific region (Whitney and Hobgood 1997), and possibly the phase of the equatorial QBO in the tropical lower stratosphere. ENSO is known to strongly modulate both the SSTs and vertical wind shear on seasonal time scales (Whitney and Hobgood 1997). Multidecadal fluctuations in ENP activity are less well understood, but show a strong relationship to the phase of the tropical multidecadal signal (Bell and Chelliah 2006) and Atlantic hurricane activity.

El Niño typically favors an above-normal ENP season, while La Niña favors a below-normal season (NOAA 2007). These ENSO impacts are modulated by the multidecadal signal, with the combination of La Niña during an inactive hurricane era (as was seen during 2007) greatly increasing the probability of a below-normal season. During 2007, the development and subsequent strengthening of La Niña during ASO led to below average SSTs (–0.5° to 1.5°C below average) in the MDR[3] during the latter half of the season

[3] For the eastern North Pacific basin the MDR covers the area 10°–20°N and 90°–130°W (green boxes, Fig. 4.18).

(Figs. 4.2c,d). Another major contributing factor to the below-normal season was above-average vertical wind shear between 200–850 hPa in the MDR throughout the season. The largest shear anomalies (exceeding 9–12 m s^{-1}) were observed during JJA (Fig. 4.18, top), followed by anomalies of 3–6 m s^{-1} during SON (Fig. 4.18, bottom).

Previous studies have shown some statistically significant correlations between ENP hurricane activity and the phase of the QBO (Gray 1984; Shapiro 1989; Whitney and Hobgood 1997). In the ENP, TCs may attain a higher intensity when the QBO is in its westerly phase at 30 hPa, but there is also a corresponding decrease in the observed seasonal frequency (Whitney and Hobgood 1997).

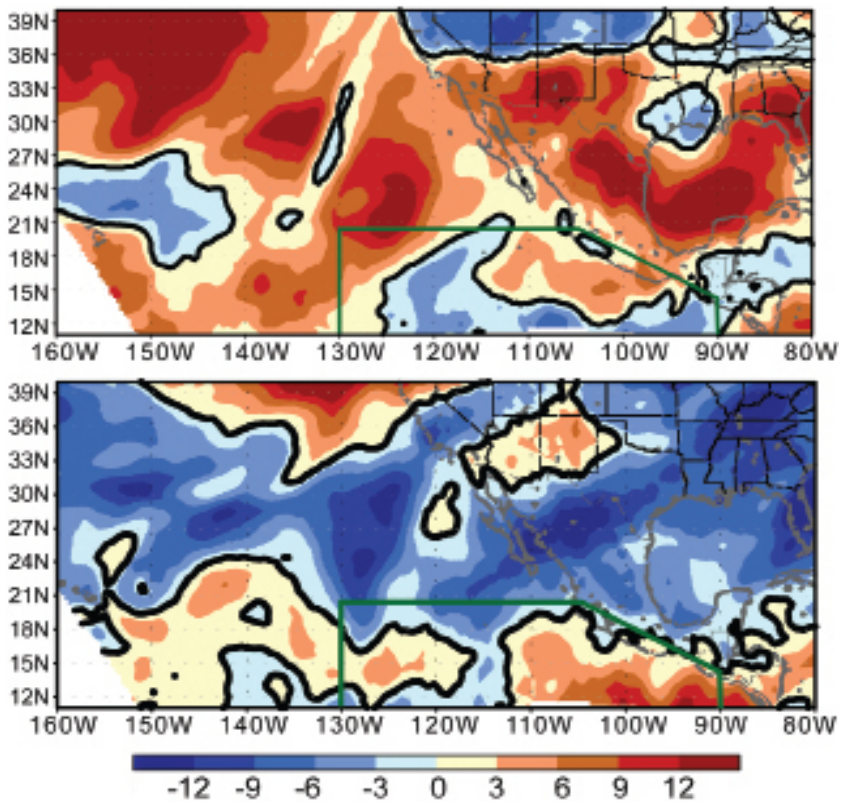

Fig. 4.18. The 200–850 hPa vertical wind shear anomaly (m s^{-1}) during (top) Jun–Aug and (bottom) Sep–Nov 2007. The green polygon shows the MDR for ENP hurricanes. Anomalies are departures from the 1979–2004 period means. [Source: NOAA NOMADS NARR dataset.]

During May, the phase of the QBO was in transition from westerly to easterly, as indicated by easterly winds at 30 hPa and westerly winds at 50 hPa. The winds were easterly at both levels in June, and subsequently strengthened over the remainder of the hurricane season (not shown). Therefore, the transition to the easterly phase of the QBO may have aided in inhibiting TC intensification in the ENP basin in 2007.

(iv) TC Impacts in 2007

Two TCs made landfall along the Pacific coast of Mexico during 2007, one as a NS (Barbara) and one as a category 1 H (Henriette). These values are close to the 1951–2000 averages of 1.34 landfalling TS and 1.3 landfalling H (Jauregui 2003).

Tropical Storm Barbara made landfall along the Mexico–Guatemala border on 2 June with maximum sustained winds of 40 kt. Damages exceeding $50 million (U.S. dollars) resulted from agricultural crop loss, downed trees, a destroyed bridge, and roof damage.

Hurricane Henriette then made landfall east of Cabo San Lucas on 4 September with sustained winds of ~70 kt. Henriette then weakened to a tropical storm, moved over the Gulf of California on 5 September, and made a second landfall on the Mexican mainland with sustained winds of 60 kt. Henriette then weakened rapidly and dissipated over the mountains of northwest Mexico. Media reports attributed nine fatalities to Henriette, and estimated damages in the Mexican state of Sonora exceeded $275 million (U.S. dollars).

There were no direct landfalls or strikes associated with the two TCs in the central North Pacific. Cosme weakened to a TD just prior to crossing 140°W on 19 July, and moved almost directly westward before dissipating on 22 July. Showers and thunderstorms north of Cosme produced 100–180 mm of rain during 20–21 July in some areas along the east and southeast slopes of the Big Island of Hawaii.

Major Hurricane Flossie with maximum sustained winds of 110 to 120 kt crossed into the central North Pacific on 11 August. Fortunately, strong vertical wind shear weakened Flossie to a tropical storm on 14 August as it passed ~160 km (~100 miles) south of the Big Island. Tropical storm force winds were observed at South Point (the southern most point of Hawaii), but no heavy rainfall, significant damage, or injuries were reported. Flossie also generated large waves along the southeast facing shoreline, with the

largest waves estimated near ~6 m. Flossie eventually weakened to a TD on 15 August as it passed south of the islands of Oahu and Kauai.

4) Western North Pacific basin—S. J. Camargo

(i) Seasonal activity

Tropical cyclone data for the WNP basin is obtained from the JTWC best-track dataset for 1945–2006 (Chu 2002), and from the JTWC preliminary operational data for 2007. The 2007 season featured 26 TCs (includes TDs), with 23 becoming NSs, 15 becoming TY, and 4 reaching STY intensity (sustained winds ≥ 130 kt).[4]

The numbers of TCs were in the bottom quartile of the distribution (Fig. 4.19a), and well below the 1971–2000 median values of 30.5 TCs, and 26.5 NSs. The number of TYs and STYs were near median (16 and 3, respectively).

It is important to note that the RSMC in Tokyo—responsible for naming the TCs—identified 5 TCs that the JTWC did not issue any warnings or advisories on: 3 TDs in July and 2 NSs in October (Haiyan and Podul). Additionally, NS 06W was considered as having NS intensity by JTWC but no name was assigned by RSMC Tokyo (Padgett 2008; Chan 2008).

The cumulative distribution of NSs shows below-normal activity throughout the season (Fig. 4.19b), and also shows many months with NSs being at or below the 25th percentile of occurrences (Fig. 4.19c). Only November featured a considerably above normal number of NSs (4). The most suppressed period was April–June, which featured 1 TC in both April and May and no TCs in June. This activity is in lowest 10th percentile of occurrences, and reflected a very slow start to the season. Interestingly, for the first time since 1969, no NSs formed in June anywhere over the entire North Pacific (Padgett 2008).

The 2007 ACE Index for the western North Pacific (Bell et al. 2000) was below the 25th percentile (Fig. 4.20a), with most months having ACE values below the climatological median (Fig. 4.20b). This suppressed activity reflects fewer and shorter-lived TCs, which is typical of a La Niña year (Wang and Chan 2002; Camargo and Sobel 2005; Camargo et al. 2007a). For example, the median lifetime of a named storm during La Niña is 6.75 days, compared to 8.25 days for ENSO-neutral years, and 9.5 days for El Niño years.

During 2007, the median named storm duration was only 4.5 days. The duration of 14 TCs was in the bottom quartile of the distribution, and only 3 TCs had lifetimes above the median (8 days). As a result, the number of days with NS storms was only 97.5 (median is 144.23), which is the second lowest value in the historical record. Only 1950 featured fewer NS days (79.5). Also, there were only 87 typhoon days in

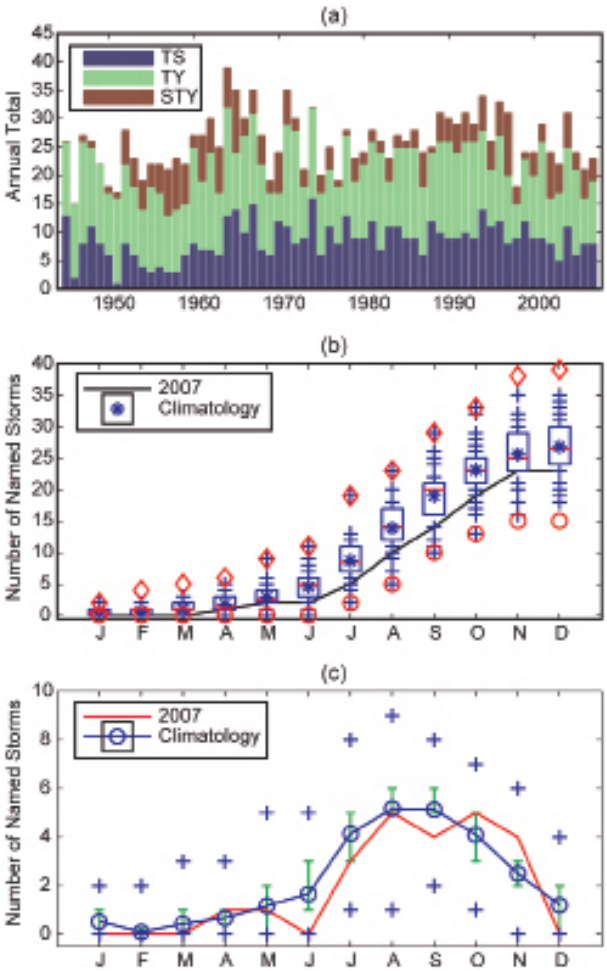

Fig. 4.19. WNP: (a) annual number of TSs, TYs, and STYs during 1945–2007. (b) Cumulative number of NSs with at least tropical storm intensity during 2007 (black line), and climatology (1971–2000). Boxes show the interquartile range, red line shows the median value, blue asterisks show the mean, blue crosses show values in the top or bottom quartile, and red diamonds (circles) show high (low) records in the 1945–2007 period. (c) Observed number of NS per month during 2007 (black curve) and climatology (blue curve). Blue "plus" signs denote the maximum and minimum monthly historical values, and green error bars show the interquartile range for each month. In the case of no error bars, the upper and/or lower percentiles coincide with the median. [Source: 1945–2006 JTWC best-track dataset, 2007 JTWC preliminary operational track data.]

[4] See http://metocph.nmci.navy.mil/jtwc/atcr/1989atcr/pdf/backmatter.pdf.

2007 (median is 120.4), which is in the lowest quartile of the distribution, and 15.5 STY days, which is also below the median (19.4 days).

During 2007, the mean genesis location (17.0°N, 135.5°E) and mean track position (21.3°N, 130.6°E) were shifted northwest of normal (12.9°N, 143.5°E and 19.0°N, 134.2°E, respectively), which is also consistent with La Niña (Chan 1985; Chia and Ropelewski 2002).

(ii) Landfalling WNP TCs

Fifteen WNP TCs made landfall during 2007, which equals the 1951–2000 median.[5] Four systems made landfall as a TD (median is 3), four made landfall as a NS (median is 6), five struck as a TY (median is 4), and two struck as a STY, which is well above the 75th percentile of occurrences. The landfalling STYs, Sepat (August) and Krosa (September), each struck Taiwan and then made a second landfall in China.

The TYs making the greatest impact were STY Sepat and Typhoon Lekima (October). STY Sepat first affected the Philippines, producing heavy rains and flooding in Manila. In Taiwan, Sepat's high winds and heavy rain caused mudslides and large agricultural losses, while in China they caused landslides in the Fujian Province. TY Lekima brought heavy rains and destruction to the Philippine Islands, followed by a second landfall in Vietnam where it destroyed approximately 100,000 homes. Lekima's rains also caused flooding and landslides in southern China.

(iii) Environmental conditions

Key environmental conditions during the peak of the WNP season (JASO) were consistent with La Niña. In particular, above average SSTs were confined to the western equatorial Pacific (Figs. 4.2c,d), the eastern portion of the monsoon trough was confined to a small region east of the Philippines (Fig. 4.21a), and anomalously high vertical wind shear was present along the equator near the date line (Fig. 4.21b). These conditions led to a northwest shift in the genesis and track activity, with most TCs also being shorter lived and weaker than normal (Wang and Chan 2002; Camargo and Sobel 2005; Camargo et al. 2007a).

The GPI (Emanuel and Nolan 2004) during 2007 was above normal in the western portion of the North Pacific and below-normal near the date line, which is also consistent with the presence of La Niña (Camargo et al. 2007b, their Fig. 6a). The decreased GPI near the date line is attributed mainly to the low-level vorticity, with some contribution from the vertical shear and midlevel relative humidity at 600 hPa. The increased GPI near the Asian continent is attributed mainly to an increase in relative humidity (Camargo et al. 2007b).

5) Indian Ocean Basins—K. L. Gleason

(i) North Indian Ocean

The NIO TC season typically extends from April to December, with two peaks in activity during May–June and November when the monsoon trough is positioned over tropical waters in the basin. Tropical cyclones in the NIO basin normally develop over the Arabian Sea and Bay of Bengal between latitudes 8° and 15°N. These systems are usually short lived and relatively weak, and often quickly move into the Indian subcontinent. However, strong and "severe cyclonic storms"[6] can develop with winds exceeding 130 kt (Neumann et al. 1993).

[5] Here we consider only one landfall per TC. If a TC makes more than one landfall, the landfall event with the highest wind speed is considered.

[6] The Bangladesh supercyclone of 1970 produced perhaps the greatest human death toll (300,000 persons) on record, primarily from storm surge flooding of low-lying deltas (Holland 1993).

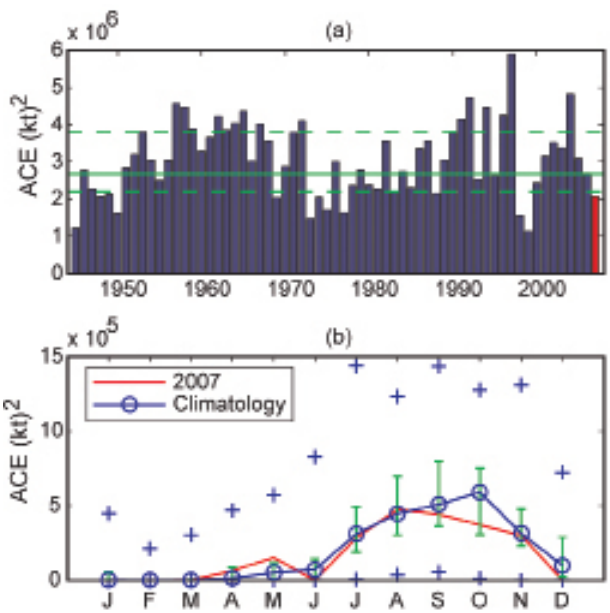

Fig. 4.20. (a) Annual ACE index for the western North Pacific. The solid green line indicates the 1971–2000 median value, and dashed green lines show the 25th and 75th percentiles. (b) Monthly ACE index during 2007 (red line), with the median (blue line) and 25th and 75th percentiles (green lines) also shown. In the case of no error bars, the upper and/or lower percentiles coincide with the median. The blue "plus" signs denote the maximum and minimum values during 1945–2007. [Source: 1945–2006 JTWC best-track dataset, 2007 JTWC preliminary operational track data.]

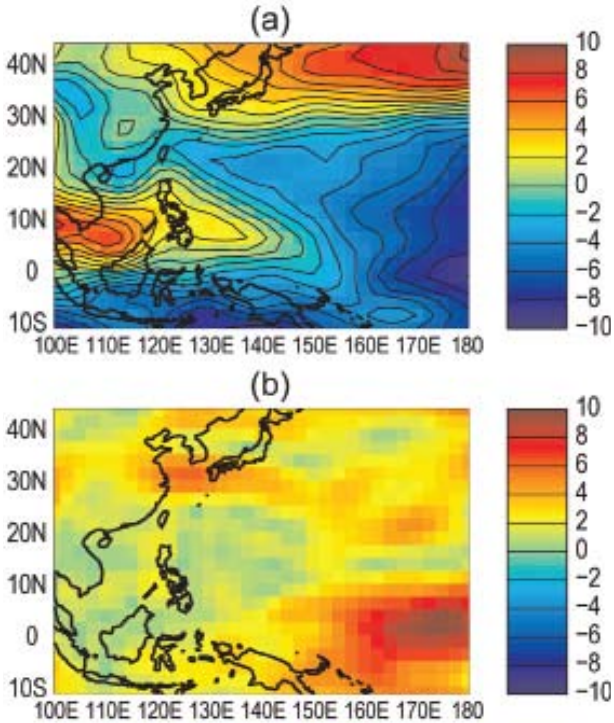

Fig. 4.21. (a) Zonal 850-hPa winds (m s^{-1}) during JASO 2007. The contour interval is 1 m s^{-1}. (b) Anomalous magnitude of the vertical wind shear (200–850 hPa) during JASO 2007. Anomalies are departures from the 1971–2007 climatological means. [Source: NCEP Reanalysis data, Kalnay et al. (1996).]

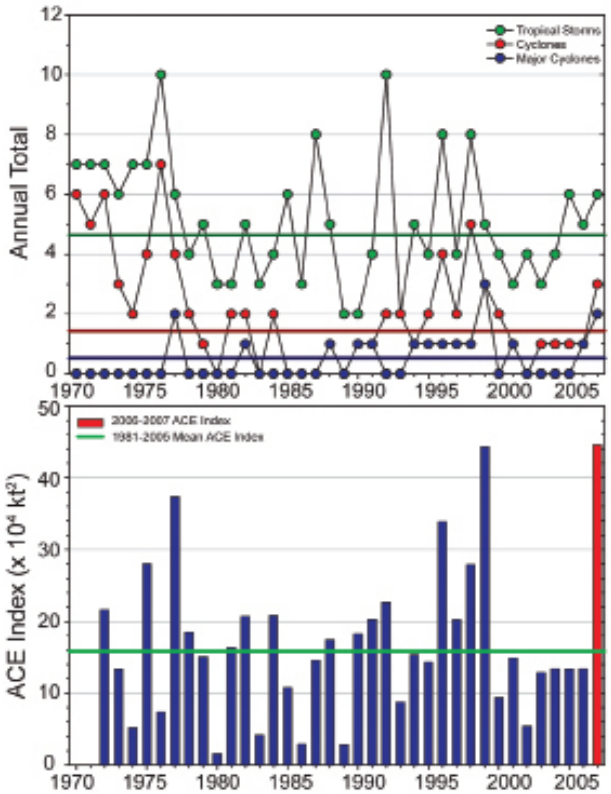

Fig. 4.22. Annual TC statistics for the NIO: (a) number of TSs, CYCs, and MCYCs, and (b) estimated annual ACE index (x 10^4 kt^2) for all TCs during which they were at least tropical storm or greater intensities (Bell et al. 2000). The 1981–2005 base period means are also shown. The ACE Index is estimated due to the lack of consistent 6-h sustained winds for every storm.

The 2007 TC season produced six NSs, three CYCs, and two MCYCs (Fig. 4.22a). These values are above the 1981–2005 averages of 4.6 NSs, 1.4 CYCs, and 0.5 MCYCs. The season also produced a record high ACE index value (44 × 10^4 kt^2), eclipsing the previous high ACE set in 1999 when a record three MCYCs formed (Fig. 4.22b). The 2007 ACE is almost 3 times the 1981–2005 mean (16 × 10^4 kt^2), and breaks a string of seven consecutive years with near- or below-average ACE.

The 2007 season was most noted for MCYCs Gonu and Sidr (see sidebar). Another storm of interest was CYC Akash, which made landfall near the Bangladesh–Myanmar border on 15 May with maximum sustained winds of 65 kt. This storm triggered a 1.2-m (4 ft) storm surge that impacted coastal areas, destroyed crops, and damaged hundreds of homes. Akash was responsible for at least three deaths and many missing persons.

(ii) South Indian Ocean

The SIO basin extends south of the equator from the African coastline to 105°E, with most CYCs developing south of 10°S. The SIO TC season extends from July to June encompassing equal portions of two calendar years (e.g., the 2007 season is composed of storms from July to December 2006 and January to June 2007). The peak activity occurs during December–April when the ITCZ is located in the Southern Hemisphere and is migrating equatorward. Historically, the vast majority of the landfalling CYCs in the SIO impact Madagascar, Mozambique, and the Mascarene Islands, including Mauritius and Réunion.

The historical SIO TC data are probably the least reliable of all the TC basins (Atkinson 1971; Neumann et al. 1993), primarily due to a lack of historical record keeping by individual countries and centralized monitoring agency; however, the historical dataset for the region has been updated (Neumann 1999). The historical data are especially deficient before reliable satellite data in the region beginning about 1983.

The 2006–07 season produced 10 NSs and well above-average numbers of CYCs (8) and MCYCs (6) (Fig. 4.23a). The 1981–2005 averages are 11.8 NSs, 6.4 CYCs, and 3 MCYCs. However, the 2006–07 ACE index (109×10^4 kt^2) was near the 1981–2005 average (Fig. 4.23b). Over the last 10 yr, only the 2001–02 season had above average ACE. Previous to that, the most recent period with above average ACE occurred during the period from 1994 to 1997.

One significant landfalling storm during the 2006–07 season was MCYC Bondo, which reached peak strength of 120 kt on 19 December, and then weakened somewhat before brushing the northern tip of Madagascar on 23 December. Most of the damage and casualties associated with Bondo occurred on Farquhar Atoll and the island of Agalega while the storm was northeast of Madagascar. Bondo then paralleled the Madagascar coastline as it continued to weaken, and made landfall near Mahajanga on 25 December as a strong NS.

The strongest storm of the season was Favio, which produced heavy rains and displaced over 25,000 people in Madagascar. Favio then intensified to a peak intensity of 125 kt after moving west of Madagascar's southern tip on 19 February. MCYC Favio then struck Mozambique's Inhambane province near Vilanculos on the 22 February with maximum sustained winds near 110 kt. At least four deaths and 70 injuries were reported.

A third significant storm of the season was MCYC Gamede, which reached a peak strength of 100 kt. Gamede did not make landfall, but did produce a record 5,510 mm (217 in.) of rain during the period from 21 to 28 February at Cratére Commerson on Réunion Island. This amount broke all world records for rainfall for a "3–8 day" period. Most of the previous records were set during TC Hyacinthe in January 1980 (Chaggar 1984).

MCYC Indlala, another significant landfalling storm, reached peak intensity of 115 kt on 14 March. MCYC Indlala struck near Antalaha, Madagascar, on 15 March with maximum winds near 105 kt. The storm resulted in more than 80 fatalities and left over 100,000 people homeless. Indlala was the fourth CYC in as many months to affect Madagascar.

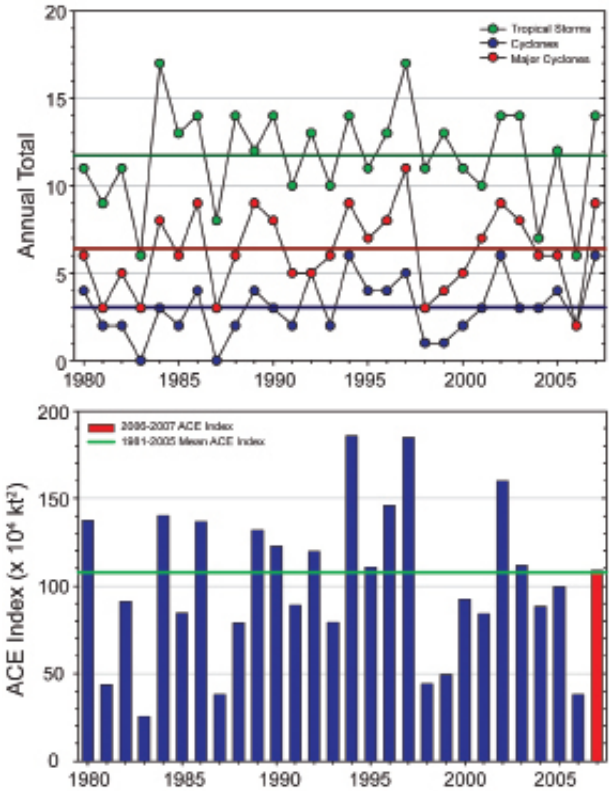

Fig. 4.23. Same as in Fig. 4.22 but for TCs in the SIO.

6) Southwest Pacific basin—M. J. Salinger and S. M. Burgess

The TC season in the southwest Pacific normally runs from November through April.

The southwest Pacific (east of 150°E) experienced seven TCs during the 2006–07 season, two less than the long-term average (Fig. 4.24). They were evenly distributed across the basin, with four TCs west of the date line and three east of the date line. Four of these systems became NSs and one became a major TC (Fig. 4.25).

The first TC of the season (Xavier) occurred on 22 October, making this the earliest start to the TC season since that of 1997, in addition Xavier reached MCYC status with sustained winds of 115 kt. Such an early start is consistent with El Niño conditions. However, the El Niño dissipated earlier than expected in January, having a dampening effect on the total number of TCs over the remainder of the season. The last TC of the season (Pierre) occurred unusually late in May. Rather than the normal February–March peak, there was a fairly even distribution of TCs throughout the season; February was unusually quiet, with no occurrences.

Significant landfalling storms included Zita and Arthur, the first TCs of the 2006–07 season, which had maximum sustained winds of 50 and 65 kt, respectively. These storms produced wind damage and coastal flooding in parts of southern French Polynesia during 23–26 January.

Tropical Cyclone Becky developed in the Coral Sea south of the Solomon Islands on 26 March and

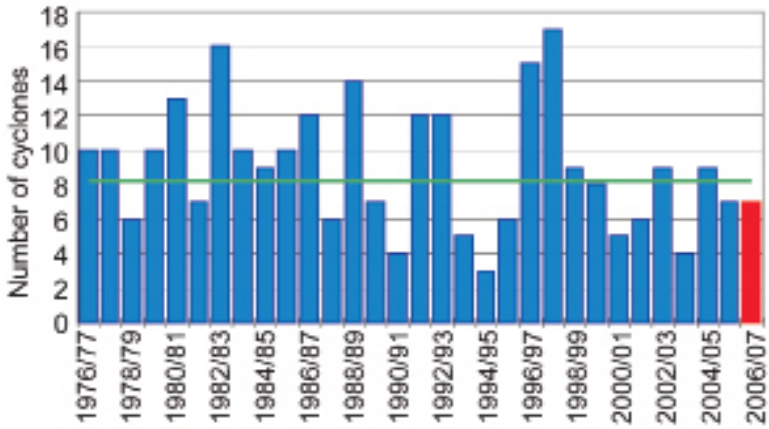

Fig 4.24. Tropical cyclones frequencies in the southwest Pacific from 1976 to 2007.

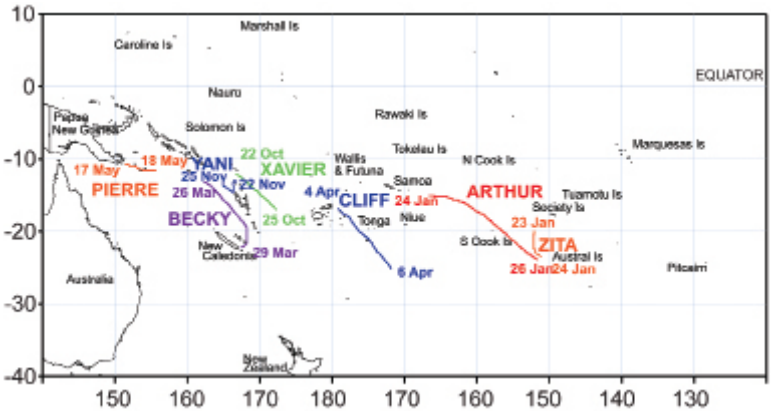

Fig. 4.25. Tropical cyclone tracks in the southwest Pacific during 2007.

reached maximum sustained winds of 70 kt. Becky tracked toward Vanuatu and then veered south toward New Caledonia. Fortunately, Becky dissipated on approach to New Caledonia, the highest wind gust reaching nearly 50 kt there. In Vanuatu, there were fallen trees and damage to crops in Espiritu and Malakula.

Tropical Cyclone Cliff occurred over the east of Fiji and Southern Tonga during 4–6 April, with maximum sustained winds of 55 kt. Some eastern parts of Fiji suffered minor wind damage and minor-to-moderate flooding. Tropical Cyclone Pierre was the last system of the 2007 season, occurring over the southeast of Papua New Guinea and the sea area south of the Solomon Islands during 17–18 May.

7) Australian basin—B. Trewin and A. B. Watkins

(i) Seasonal activity

The 2006–07 TC season was notably below normal in the broader Australian basin (areas south of the equator and between 90° and 160°E,[7] which include Australian, Papua New Guinea, and Indonesian areas of responsibility). The season produced five TCs, which is well below the long-term average of 10. This activity is the equal lowest since at least 1943–44. Historically, TC activity in the Australasian region, especially the Pacific region, is most suppressed during El Niño. There were only two TCs in the eastern sector[8] of the Australian region during 2007 and three TCs in the western sector. The inactive season coincided with a late monsoon onset over northern Australia, which was delayed by two weeks until mid-January, and also with long periods of below-average tropical convection over Indonesia and northern Australia (Fig. 4.5).

(ii) Landfalling TCs

MCYC George was the most significant system of the season, forming on 3 March off the west coast of the top end of the Northern Territory, and ultimately made landfall on 8 March as an Australian category 5 (see www.bom.gov.au/weather/cyclone/faq/index.shtml for a definition of Australian TC categories) storm 50 km ENE of Port Hedland. George weakened slowly after landfall (Fig. 4.26), and was still an Australian category 2 system late on 9 March. The remnant low finally dissipated on 12 March between Giles and Laverton in the western Australian interior.

George caused widespread minor-to-moderate damage in Port Hedland, with the most severe damage and three deaths occurring in mining camps south and east of town. Bedout Island recorded a 10-min mean wind of 105 kt (equivalent to wind gusts of approximately 150 kt). It was the most significant impact in the town since 1975. Fortunately, there was

[7] The Australian Bureau of Meteorology's warning area overlaps both the SIO and SWP.

[8] The western sector covers areas between 90° and 125°E. The eastern sector covers areas east of the eastern Australian coast to 160°E, as well as the eastern half of the Gulf of Carpentaria. The northern sector covers areas from 125°E east to the western half of the Gulf of Carpentaria.

no significant storm surge on the populated coastline, and no substantial flood damage in western Australia. However, heavy rains from the precursor low pressure system in late February and early March caused significant flooding in the Northern Territory.

Another landfalling storm was TC Nelson, which caused some flooding north of Karumba on the east coast of the Gulf of Carpentaria on 6 February. Tropical Cyclones Jacob and Kara were important in that they both caused major disruption to offshore oil and gas operations as platforms were evacuated in advance of the approaching systems. The remnants of TC Jacob crossed the coast on 12 March in almost exactly the same location that MCYC George had struck four days earlier.

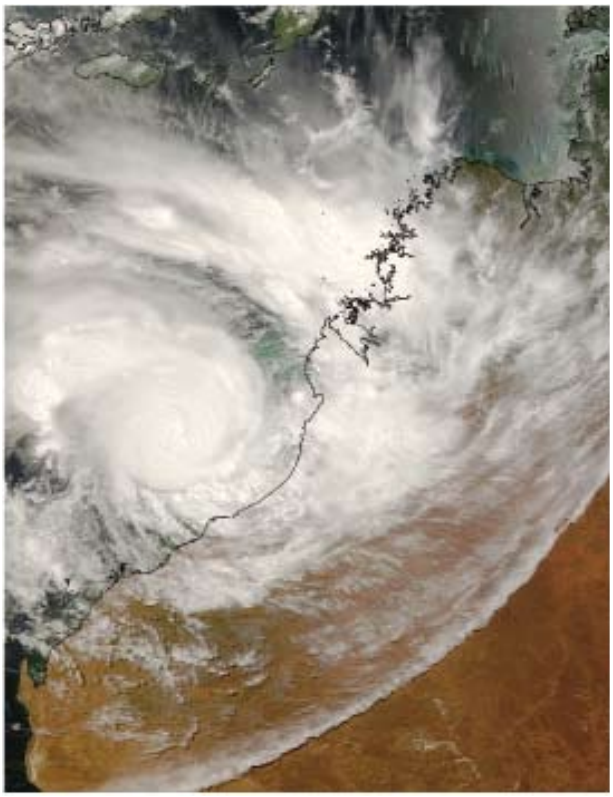

Fig. 4.26 Tropical Cyclone George approaching the coast of western Australia at 0155 UTC, 8 Mar 2007. [Courtesy of MODIS Rapid Response Project at NASA's Goddard Space Flight Center.]

e. Intertropical convergence zones

1) Pacific ITCZ—A. B. Mullan

There are two prominent convergence zones in the Pacific: the ITCZ in the Northern Hemisphere between 5° and 10°N, and the SPCZ that extends southeastward from near the Solomon Islands (10°S, 160°E) to near 30°S, 140°W. The Southern Hemisphere counterpart to the ITCZ also occurs near 5°S, but is seen mainly during February through April and east of the date line. This feature is suppressed or absent during El Niño years when warmer waters near the equator disrupt the seasonal convergence patterns. During 2007, the Pacific convergence zones reflected the transition from weak El Niño conditions early in the year to a moderate La Niña by the end of the year (section 4b).

The ITCZ appears as a fairly broad feature in the annual mean pattern of tropical rainfall due to its normal meridional movement throughout the year (Fig. 4.27, top). However, in 2007 the ITCZ was closer to the equator than normal at the beginning of the year in association with El Niño, and farther poleward than normal later in the year due to La Niña (Fig. 4.28). A double ITCZ was present from the second half of February through April and, although it appears weak in the annual mean, was nearly as intense as the northern branch during March 2007. West of the date line where the ITCZ and SPCZ tend to merge, the annual rainfall totals were comparable to the 1998–2006 TRMM climatology.

The SPCZ was shifted equatorward and eastward of normal in January consistent with El Niño, and produced enhanced convection from north of the Solomon Islands to central French Polynesia (Fig. 4.27, bottom). Penrhyn, in the northern Cook Islands, recorded its second highest January rainfall on record (262% of normal). At the same time, the Caroline Islands of northern Micronesia experienced dry conditions through March 2007 (Fig. 4.28). The SPCZ was particularly active in March between 180°–150°W, producing record rainfall in Niue, Tonga, and some of the northern Cook Islands.

Although the National Aeronautics and Space Administration's ENSO Precipitation Index (Curtis and Adler 2000) was persistently negative and consistent with La Niña from March–December 2007, the convergence zones did not stray from their climatological positions until July. The northward displacement of the ITCZ first occurred in the far eastern equatorial Pacific (120°–90°W) in July and then extended to the central Pacific during September (Fig. 4.29).

2) Atlantic ITCZ—A. B. Pezza and C. A. S. Coelho

The Atlantic ITCZ is a well-organized convective band that oscillates between 5° and 12°N during July–November, and between 5°N and 5°S during January–May (Waliser and Gautier 1993). The Atlantic ITCZ is active throughout the year, demarcating the transition from the southeasterly to the northeasterly Atlantic trade winds. Its positioning

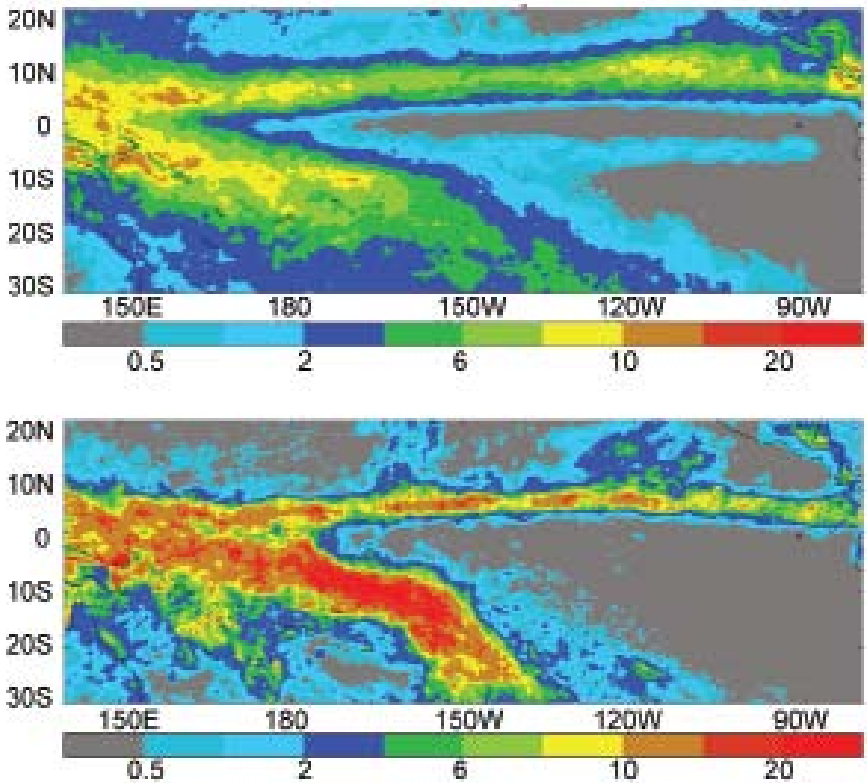

Fig. 4.27. Average rainfall rate (mm day^{-1}) during (top) 2007 and (bottom) Jan 2007. Note the uneven contour intervals (0.5, 1, 2, 4, 6, 8, 10, 15, and 20 mm day^{-1}). Data are NASA TRMM estimates (3B-43 product) provided on a 0.25° lat–lon grid.

modulates the rainy seasons of northern and northeastern South America and northwestern Africa. In northeastern Brazil where annual rainfall is low, an occasional southward burst can produce widespread heavy rains (Fig. 4.30).

The seasonal migration and zonally asymmetric structure of the Atlantic ITCZ are primarily driven by land–sea temperature contrasts, low-level winds, moisture convergence, and the meridional SST gradient between the North and South Atlantic (Nobre and Shukla 1996). Large-scale dynamics associated with equatorial atmospheric Kelvin waves can also influence the interannual variability of the ITCZ, while ENSO can influence its seasonal variability (Münnich and Neelin 2005).

During 2007 the Atlantic ITCZ reached its southernmost position (2.5°S) in early May (Fig. 4.31b), which is slightly later than the climatological period of March/April (Waliser and Gautier 1993). This delay may partly be a lagged response to the demise of the 2006 El Niño event (Münnich and Neelin 2005). The ITCZ also displayed some erratic southerly bursts during the year. A major event in February (Fig. 4.31a) produced enhanced rainfall across northeastern Brazil, with the

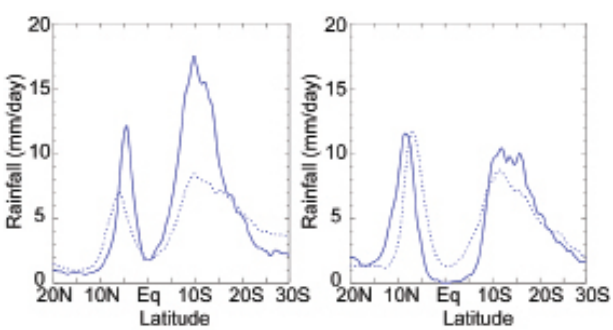

Fig. 4.28. Latitudinal cross sections of TRMM rainfall (mm day^{-1}) averaged between 180° and 150°W during (a) Jan and (b) Dec 2007. Solid (dotted) lines indicate the profiles for 2007 (1998–2006 average).

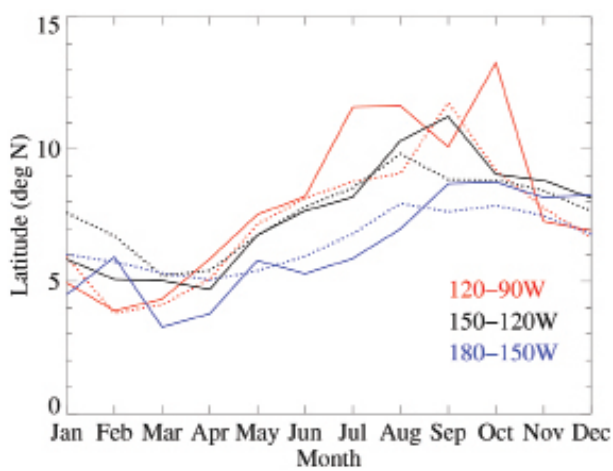

Fig. 4.29. Monthly variation in latitude of peak ITCZ rainfall over three longitude sectors: 180°–150°W (blue), 150°–120°W (black), and 120°–90°W (red). Solid (dotted) lines show annual cycle variations during 2007 (1998–2006 average).

largest surpluses exceeding 300 mm (Fig. 4.30). Enhanced precipitation during this period also extended well to the south due to interactions with cold fronts.

For the remainder of the year the Atlantic ITCZ either oscillated around its mean latitudinal position or stayed anomalously to the north. Its northernmost position occurred along the eastern flank in July and August, which produced strong convection over the western tip of Africa between 10° and 15°N (Fig. 4.31c). As a result, a large area of the tropical South Atlantic recorded less rainfall in 2007 than the 1998–2006 annual mean (Fig. 4.32), similar to what was observed in 2006.

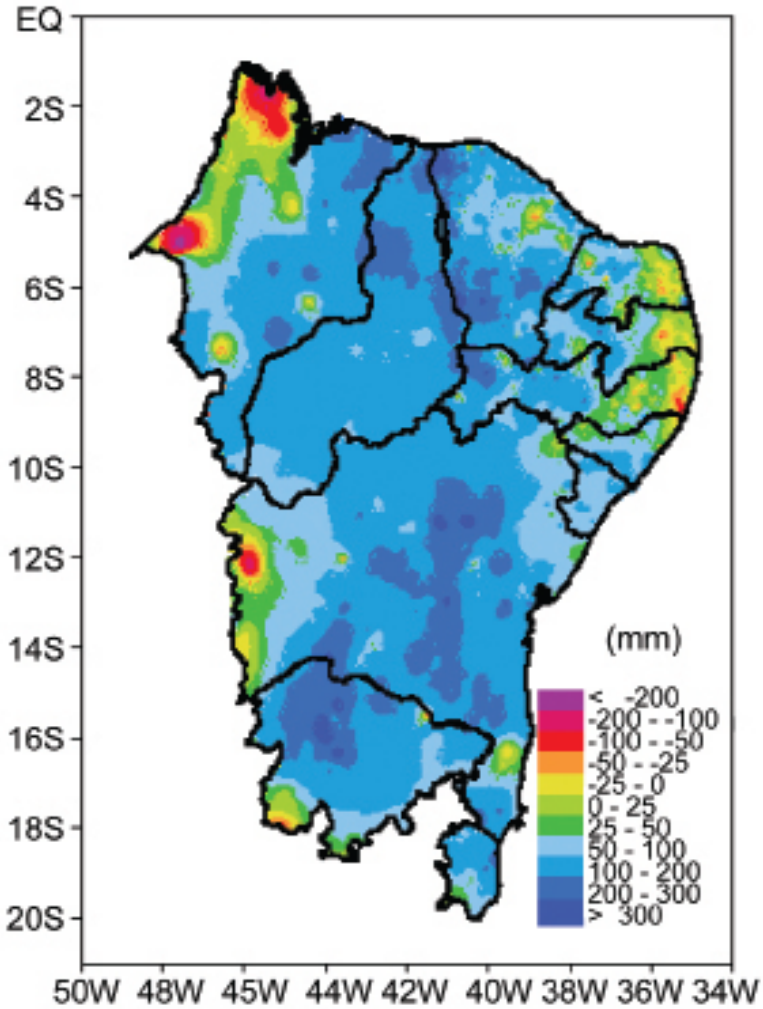

Fig. 4.30. Northeastern Brazil precipitation anomalies (mm) during Feb 2007. Anomalies are departures from the 1961–90 base period monthly means. [Data source: federal and regional networks (CMCD/INPE, INMET, SUDENE, ANEEL, FUNCEME/CE, LMRS/PB, EMPARN/RN, ITEP/LAMEPE/PE, CMRH/SE, SEAAB/PI, SRH/BA, CEMIG/SIMGE/MG, SEAG/ES).]

f. Indian Ocean dipole—J. J. Luo and G. D. Bell

The IOD is an El Niño–like air–sea coupled ocean–atmosphere climate phenomenon in the tropical IO (Saji et al. 1999; Webster et al. 1999). It usually develops during JJA, peaks during SON, and decays during December and January, undergoing a strong phase-locking with the East Asian–Australian monsoon winds. The IOD signal can intensify quickly through air–sea interactions, and its intrinsic period is approximately two years. The duration is mainly controlled by a delayed negative feedback transmitted in the IO subsurface temperature (Behera et al. 2006).

The pIOD features anomalously cool SSTs and a shallower than normal oceanic thermocline along the west coast of Sumatra, and anomalously warm SSTs and a deeper than normal thermocline in the western IO. Despite the fact that the IOD signal is usually weak compared to El Niño, its related SST anomalies in the warm IO may cause large climate anomalies, particularly in the Eastern Hemisphere. For instance, the strong pIOD event in 2006 boreal fall, which was coincident with a weak El Niño, caused considerable impacts in Australia, East Asia, Indonesia, and East Africa (Luo et al. 2008).

During 2007, a pIOD signal began during August in association with anomalous low-level southeasterly winds extending from west of Sumatra to the central equatorial IO (Fig. 4.33a). The initial SST cooling occurred along the Java Coast, followed by stronger negative anomalies (–1°C) in September near the Sumatra–Java coast (Fig. 4.33b). The cold signal then dissipated in mid-November, making it a relatively short-lived event. This early decay was partly linked to the downwelling phase of an oceanic Kelvin wave that was triggered in the west-central equatorial IO by westerly wind anomalies associated with the MJO.

The 2007 IOD probably contributed to drought in the eastern IO, Indonesia, and southeastern Australia, and floods in the western IO, South India, and East Africa. Drought damage estimates in Victoria, Australia alone were estimated at $2 billion (Australian

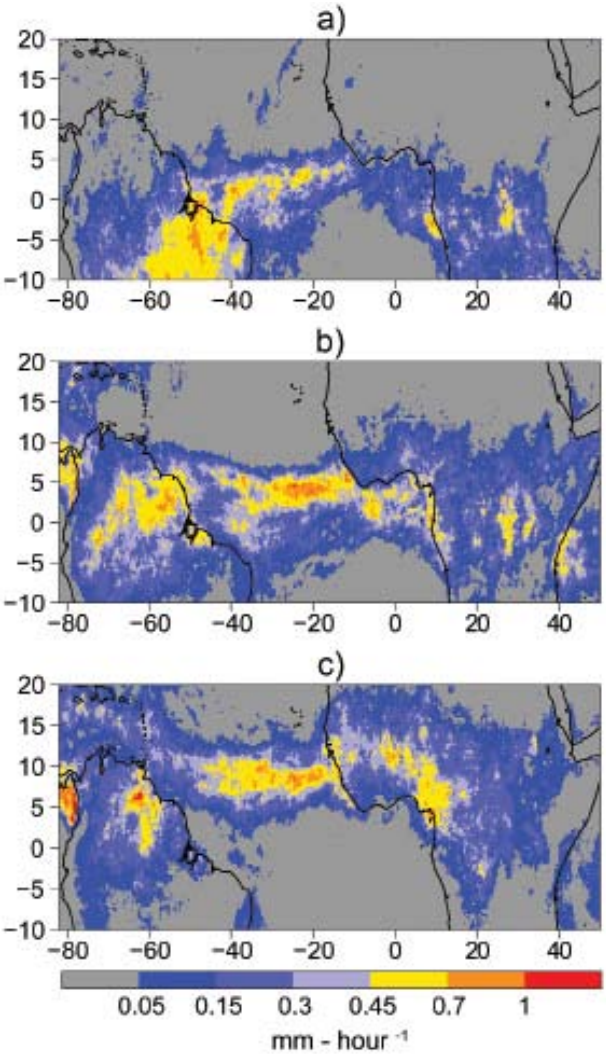

Fig. 4.31. Average rainfall rate (mm h^{-1}) during (a) Feb, (b) May, and (c) Aug 2007. Data are TRMM estimates calculated from a 0.25° lat–lon grid.

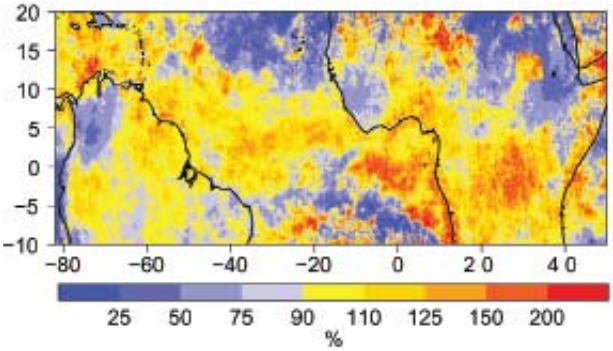

Fig. 4.32. Percentage of the 1998–2006 mean annual rainfall during 2007. Data are TRMM estimates calculated from a 0.25° lat–lon grid.

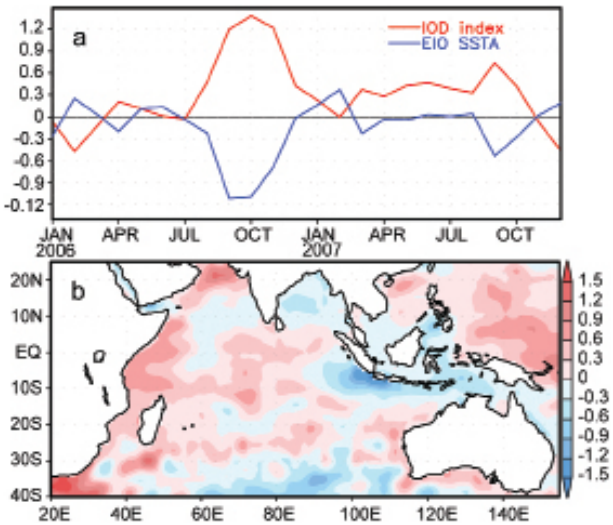

Fig. 4.33. (a) Monthly SST indices (°C) for the IOD and for the eastern IO (EIO) (10°S–0°, 90°–110°E). The IOD index is defined as the difference in SST anomalies between the western IO (10°S–10°N, 50°–70°E) and the EIO (Saji et al. 1999). (b) Anomalous SSTs (°C) in Sep 2007. Analysis is based on the NCEP optimum interpolation SST (Reynolds et al. 2002). Anomalies are departures from the 1982–2006 period monthly means.

dollars) (source: Australian Bureau of Meteorology). A pIOD was also present in 2006, and it is unprecedented to have consecutive positive events. Using only SSTA as a guide, the 2007 event was approximately one-half as strong as the 2006 event, which occurred during El Niño and likely contributed to the observed El Niño–related pattern of suppressed convection over Indonesia and the western tropical Pacific. That combination of conditions was associated with the climate and societal impacts described earlier (Luo et al. 2008).

The 2007 IOD event occurred during La Niña, suggesting an independence from ENSO that was also noted by Saji et al. (1999) and Saji and Yamagata (2003). As discussed in section 4diva (Fig. 4.15), the 2007 IOD was part of a much-larger, record-strength pattern of tropical convection spanning the IO, Indonesia, and southeastern Asia (Fig. 4.15b). This pattern is more typical of El Niño, meaning that the total La Niña forcing onto the upper-level atmospheric winds was weaker than would normally be expected for the observed equatorial Pacific SST anomalies.

Embedded within this pattern, the outgoing longwave radiation anomalies in the IOD region were comparable to the strongest in the record (Fig. 4.34a). The north–south dipole of anomalies between the Indian/Southeast Asian monsoon regions and the

eastern IO/Indonesian region was the strongest in the record, surpassing the previous record set in 2006 (Fig. 4.34b). The underlying mechanisms for the 2006 and 2007 pIOD events are found to differ. The 2006 event is consistent with the large-scale IOD dynamics, and was predictable at long leads due to the oceanic subsurface memory (Luo et al. 2007, 2008). However, the 2007 event was apparently triggered by active intraseasonal easterly wind anomalies during May–July in the central equatorial IO. As a consequence, that event had less predictability (Luo et al. 2008).

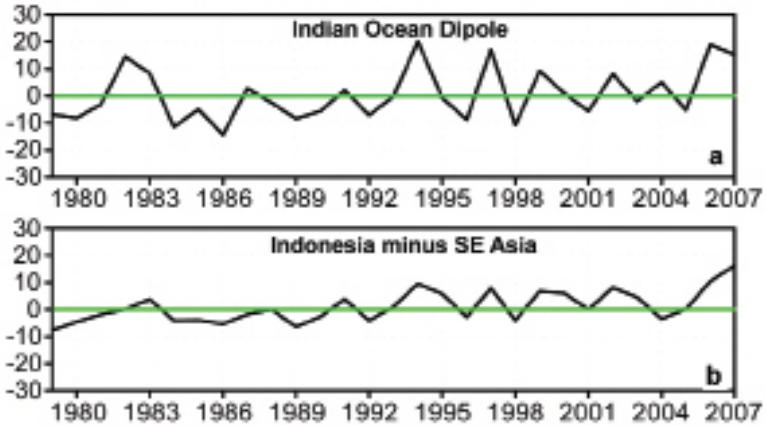

Fig. 4.34. Aug–Oct time series of OLR (W m^{-2}) anomalies based on the boxed regions in Fig. 4.15a; (a) the IOD (Indonesia minus western IO); and (b) Indonesia minus southeastern Asia. Anomalies are departures from the 1979–2000 period monthly means.

A RECORD NORTH INDIAN OCEAN TC SEASON—K. L. GLEASON AND H. J. DIAMOND

The 2007 TC season in the NIO basin featured MCYC Gonu, the strongest documented storm in the Arabian Sea, and the second strongest documented storm in the NIO. It also produced MCYC Sidr, which was perhaps the worst storm to strike Bangladesh since 1991. These two systems produced major impacts across the region (Fig. 4.35).

Tropical Cyclone Gonu developed in early June within the eastern Arabian Sea. Within three days, Gonu had strengthened to a MCYC with peak winds near 140 kt (category 5) on 4 June. The storm then weakened within an environment of cooler water and dry air prior to making landfall on 5 June along the eastern tip of Oman. Gonu struck with 80-kt sustained winds, and was the strongest CYC on record to hit the Arabian Peninsula. Gonu then entered the Gulf of Oman and made a subsequent landfall in Iran with sustained winds of 108 kt.

During a 24-h period from 6–7 June, rainfall totals were approximately 70 mm in the capital city of Muscat, Oman and surrounding stations (source: WMO Severe Weather Information Centre at http://severe.worldweather.wmo.int/). These amounts are especially significant, considering the average June rainfall in Oman is only 0.6 mm, and the mean annual rainfall is 100 mm (source: WMO World Weather Information Service). This widespread, heavy rain produced floods and landslides across coastal portions of Oman, resulting in over 50 fatalities and damages estimated at over $1 billion (U.S. dollars).

MCYC Sidr then formed near the Andaman Islands in the Bay of Bengal during mid-November. Sidr was named on 12 November, and reached maximum intensity of 135 kt on 15 November. Sidr then made landfall later that day in the Sundarbans forest area of Bangladesh as a strong category 4 storm with 130-kt winds. The storm produced heavy rains, high surf, and widespread flooding, and affected nearly 3 million people. More than 2,400 fatalities were reported, mostly attributable to collapsed buildings and flying debris.

MCYC Sidr was a category 5 storm that developed in the Bay of Bengal and became perhaps the most intense storm ever recorded in the NIO, achieving a minimum central pressure of 898 hPa with maximum sustained winds of 140 kt . It was also one of the deadliest recorded storms with over 140,000 confirmed fatalities in Bangladesh, many resulting from the 6-m storm surge in the Chittagong district.

Fig. 4.35. Satellite montage of two category 5 TCs over the NIO. [Courtesy: C. Velden, University of Wisconsin—Madison, CIMSS.]